Structure of the actively deforming fold-thrust belt of the St. Elias orogen with implications for glacial exhumation and three-dimensional tectonic processes

Terry L. Pavlis[1], James B. Chapman[1,*], Ronald L. Bruhn[2], Kenneth Ridgway[3], Lindsay L. Worthington[4,†], Sean P.S. Gulick[4], and James Spotila[5]

[1]*Department of Geological Sciences, University of Texas at El Paso, El Paso, Texas 79968, USA*
[2]*Department of Geology and Geophysics, University of Utah, Salt Lake City, Utah 84112, USA*
[3]*Department of Earth and Atmospheric Sciences, Purdue University, West Lafayette, Indiana 47907, USA*
[4]*Institute for Geophysics, J.J. Pickle Research Campus, Building 196, University of Texas at Austin, Austin, Texas 78758-4445, USA*
[5]*Department of Geosciences, Virginia Tech, Blacksburg, Virginia 24061, USA*

ABSTRACT

Previous studies in the Yakataga fold-thrust belt of the St. Elias orogen in southern Alaska have demonstrated high exhumation rates associated with alpine glaciation; however, these studies were conducted with only a rudimentary treatment of the actual structures responsible for the deformation that produced long-term uplift. We present results of detailed geologic mapping in two corridors across the onshore fold-thrust system: the Duktoth River transect just west of Cape Yakataga and the Icy Bay transect in the Mount St. Elias region. In the Duktoth transect, we recognize older, approximately east-west–trending structures that are overprinted by open, northwest-trending fold systems, which we correlate to a system of northeast-trending, out-of-sequence, probably active thrusts. These younger structures overprint a fold-thrust stack that is characterized by variable structural complexity related to detachment folding along coal-bearing horizons and duplexing within Eocene strata. In the Icy Bay transect, we recognize a similar structural style, but a different kinematic history that is constrained by an angular unconformity at the base of the syntectonic Yakataga Formation. At high structural levels, near the suture, structures show a consistent northwest trend, but fold-thrust systems rotate to east-west to northeast trends in successively younger structures within the Yakataga Formation. We present balanced cross sections for each of these transects where we project the top of basement from offshore seismic data and assume a subsurface structure with duplex systems similar to, but simplified from, structures observed in the onshore transects. These sections can account for 150–200 km of shortening within the fold-thrust system, which is <33% of the likely convergence based on the subsurface geometry of the subducted Yakutat terrane lithosphere. This mismatch with known convergence is the result of loss of the earliest thrust belt structures by erosion and recycling into the orogen, sediment subduction, and three-dimensional (3D) motions that move mass through the cross section. Based on order of magnitude estimates and regional geophysical studies, we suggest that sediment subduction has been significant and probably accounts for previously recognized low Vp/Vs (compressional to shear wave velocity) ratios in the mantle wedge above subducting Yakutat lithosphere.

Our section restorations also provide a simple explanation for the observed elongate bullseye pattern of low-temperature cooling ages in the thrust belt as a consequence of exhumation above the growing duplex and/or antiformal stack. Comparison with analog model studies suggests that structural feedbacks between erosion and development of décollement horizons in coal-bearing strata led to this structural style. Although previous studies based on thermochronology suggested an active backthrust at the northern edge of the thrust belt, section restorations indicate that a backthrust is allowable but not required by available data.

The Yakataga fold-thrust belt has been treated as a dominantly 2D system, yet our work indicates that 3D processes are prominent. In the Duktoth transect, we interpret a group of northeast-trending thrusts as younger, out-of-sequence structures formed in response to the rapid destruction of the orogenic wedge by glacial erosion and deposition immediately offshore. We infer that these northeast-trending thrusts transfer slip downdip into a duplex system that forms the antiformal stack modeled in cross-section restorations, and we infer that these structures represent thrusting stepping back from the active thrust front attempting to rebuild an orogenic wedge that is being destroyed as rapidly as, or more rapidly than, it is being rebuilt. In the Icy Bay transect, we use the relative chronology provided by an angular unconformity beneath the syntectonic Yakataga Formation to infer that early, northwest-trending fold-thrust systems were formed along the Fairweather transform as transpressional structures. Continued strike slip carried these structures into the tectonic corner between the Fairweather and Yakataga segments of the orogen, producing a counterclockwise rotation of the shortening axis until the rocks reached their present position.

INTRODUCTION

Southern Alaska (Fig. 1) contains one of the world's most rapidly deforming collisional orogens in the Wrangell–St. Elias region, but this

*Present address: SandRidge Energy Inc., 123 Robert S. Kerr Ave., Oklahoma City, Oklahoma 73102, USA.
†Present address: Department of Geology and Geophysics, Texas A&M University, College Station, Texas 77843, USA.

Geosphere; October 2012; v. 8; no. 5; p. 991–1019; doi:10.1130/GES00753.1; 13 figures; 2 plates; 3 supplemental files.
Received 14 September 2011 ♦ Revision received 25 April 2012 ♦ Accepted 8 May 2012 ♦ Published online 18 September 2012

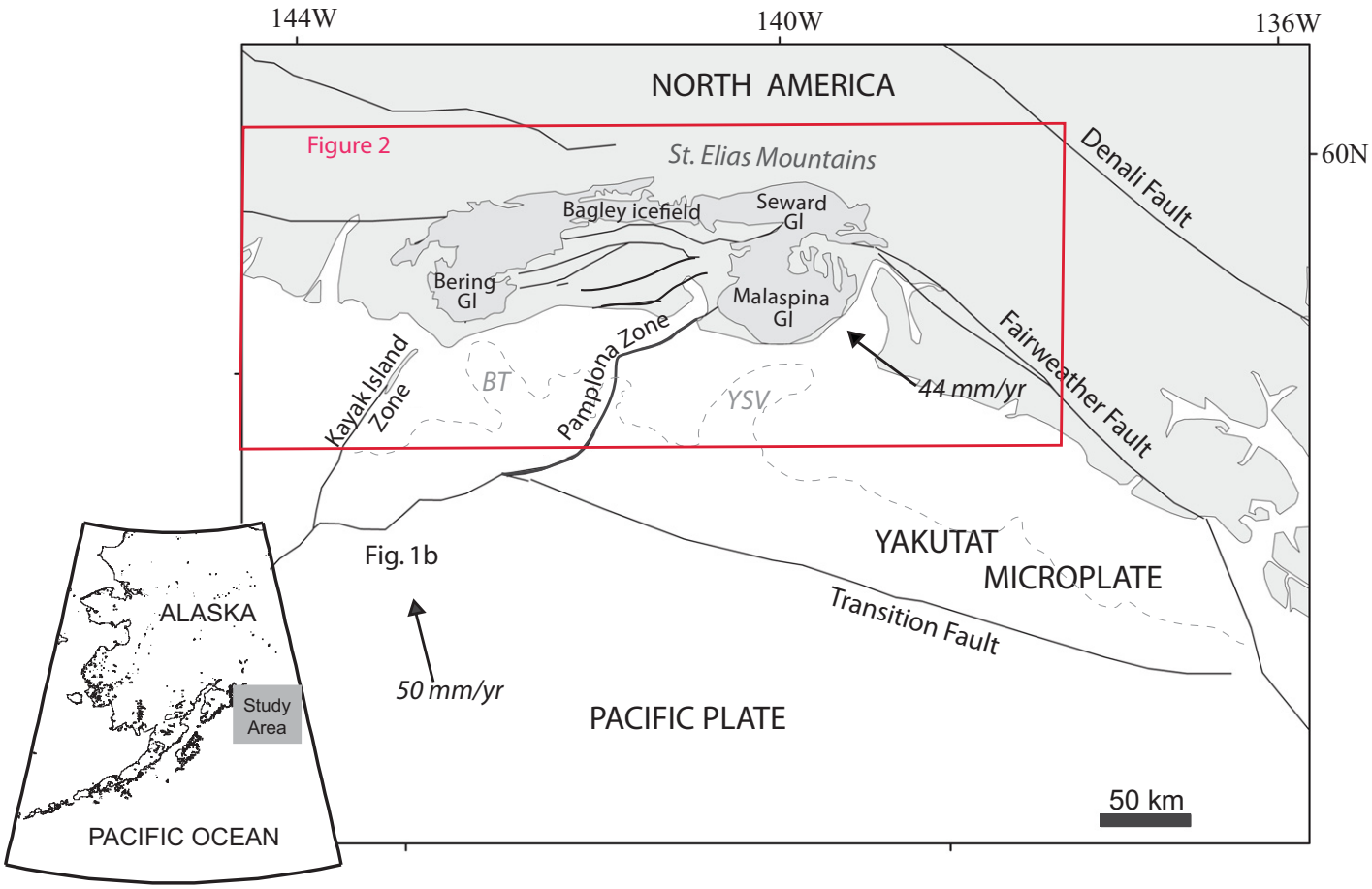

Figure 1. Regional tectonic setting of this study relative to Alaska (lower left) and the local study area (main figure) (after Worthington et al., 2010). Gl—glacier; BT—Bering Trough; YSV—Yakutat Sea Valley.

orogen is also being exhumed at some of the highest rates on Earth. The exhumation differs from most orogens, however, in that glacial and glaciofluvial erosion and deposition dominate the region. This produces the characteristic high-relief glacial terrain of southern Alaska, where high peaks tower above low valleys because focused erosion in valleys by temperate ice can keep up with, or exceed, tectonic rates, and high peaks are isolated from erosion as they rise above the polar ice limit (Griffiths, 1952). Thus, although southern Alaska contains most of North America's highest peaks, the overall elevation of the orogen is relatively low (Meigs and Sauber, 2000). This general observation is broadly consistent with the glacial buzzsaw hypothesis (e.g., Brozovic et al., 1997; Hallet et al., 1996; Montgomery, 2002; Brocklehurst and Whipple, 2002); therefore, southern Alaska has been a centerpiece in understanding interplays between erosion and tectonics in a glacially dominated system.

Exhumation rates for the St. Elias orogen have been estimated for short time scales from Holocene sediment yield studies (Hallet, 1979; Hallet et al., 1996; Jaeger et al., 1998; Sheaf et al., 2003) and for longer time scales through thermochronology (Meigs et al., 2008; Berger and Spotila, 2008; Berger et al., 2008a, 2008b; Spotila and Berger, 2010; Enkelmann et al., 2008, 2009, 2010; Gasser et al., 2011). These studies all indicate orogen-wide exhumation rates in excess of 2–3 mm/yr, an elongate area of rapid exhumation >4 mm/yr, and localized focused exhumation in excess of 10 mm/yr. Thermochronology studies show a clear correlation between very young apatite He dates (younger than 1 Ma) and the onshore fold-thrust belt with young ages concentrated outboard of the collisional suture (Fig. 2). Berger and Spotila (2008) and Berger et al. (2008a, 2008b) noted the close correlation between the area of very young ages and the average glacial equilibrium line altitude (ELA), and concluded that focused erosion at the ELA had reshaped the orogen during the late Pleistocene. A preliminary synthesis of the thermochronology data with available onshore and offshore data was developed to conclude that deformation had shifted over time within the orogen in direct response to onset of intense exhumation during the Pleistocene (Berger et al., 2008a, 2008b; Chapman et al., 2008). Recent mapping using seismic reflection data offshore of the Bering Glacier shows a distinct shift in offshore deformation at the mid-Pleistocene transition coincident with increased depositional flux to the continental shelf due to this intensified exhumation (Berger et al., 2008b; Worthington et al., 2010).

These studies offer one of the clearer examples of how changing exhumation and deposition during the history of an orogen can change the distribution of active deformation (Whipple, 2009). Despite the importance of these results, the studies were conducted with little reference to how uplift was maintained over sufficient time to produce the observed exhumation patterns. The development of out-of-sequence, en echelon thrusts within the core of the orogen was proposed in Chapman et al. (2008), based on geomorphic evidence, and Berger et al. (2008b) further proposed a backthrust based on

patterns of cooling ages. Both of these hypotheses represent potential tectonic configurations that could produce the structural feedbacks to account for the long-term exhumation. Nonetheless, these proposed mechanisms remain relatively speculative.

This paper was motivated by this question of how the internal orogenic structure accounts for the observed exhumation pattern. We begin with a summary of the structure within the core of the orogen, focusing on results of ~1:25,000-scale geologic mapping along two transects. In these descriptions, we show that three-dimensional (3D) processes have shaped the orogen and that out-of-sequence thrusts complicate simple interpretation of the structure. Although 3D structure is prominent, the deformation is sufficiently 2D that cross-section construction is informative, and we present shortening estimates from cross-section restorations. We conclude that the modern structure is dominated by the development of a regional antiform overlying a duplex beneath the site of the Pleistocene high exhumation rates. We discuss alternative scenarios and conclude that two distinct processes are fundamental to the system: (1) out-of-sequence thrusts cut obliquely across older structures, probably accommodating a component of dextral transpression in a process similar to that described in Chapman et al. (2008); and (2) complexly changing kinematics are associated with material transported through an oblique-convergent orogen into a fully convergent system in this tectonic corner (as modeled by Koons et al., 2010).

TECTONIC SETTING

The St. Elias orogen represents the collisional orogenic system that developed from Miocene to recent time along the strike-slip to subduction transition of the northern Cordilleran margin (Fig. 1). The St. Elias orogen is only part of the broader southern Alaskan orogen that spans the northern Cordilleran margin from southeast Alaska to the Alaska Peninsula (Pavlis et al., 2004; Mazzotti and Hyndman, 2002; Koons et al., 2010).

The St. Elias orogen was formed when the Yakutat terrane was excised as a strike-slip sliver from the western margin of North America and was carried northward into the Alaskan-Aleutian subduction zone (Plafker, 1987; Plafker et al., 1994). Evidence from synorogenic strata (Plafker, 1987; Plafker et al., 1994; Zellers, 1995), thermochronology (e.g., Enkelmann et al., 2008, 2010; Gasser et al., 2011), and the present extent of the subducted part of the Yakutat terrane (Ferris et al., 2003; Eberhart-Phillips et al., 2006) indicate that the leading edge of the Yakutat terrane had encountered the trench by ca. 10–12 Ma. There is some evidence, however, that the initial interaction began as long ago as the early Neogene (Enkelmann et al., 2008; Haeussler, 2008; Finzel et al., 2011; Benowitz et al., 2011; Gasser et al., 2011), assuming that the earliest cooling north of the suture is related to the collision rather than subduction zone processes.

In the core of the St. Elias orogen, the suture can be mapped relatively easily (Fig. 2) because the Yakutat terrane carries a distinctive Paleogene cover sequence that is absent from the southern Alaskan margin (Plafker, 1987). The suture, referred to as the Chugach–St. Elias fault, follows an irregular trace from a position offshore in the Copper River delta to the core of the orogen (Pavlis et al., 2004; Chapman et al., 2012). To the east of the Malaspina Glacier, however, the suture merges with the active strike-slip trace of the Fairweather fault (Fig. 2).

Outboard of the suture the sedimentary cover of the Yakutat terrane has been stripped from basement, forming a thin-skinned fold-thrust belt (Plafker, 1987). Active structures of this fold-thrust system continue offshore, where they were imaged in seismic reflection data more than 30 yr ago (Bruns and Schwab, 1983; Plafker, 1987). Seismic data collected during the St. Elias Erosion and tectonics Project (STEEP) and related efforts (Worthington et al., 2008, 2010, 2012; Berger et al., 2008b) provide a clearer picture of the offshore structure that we use extensively here.

In the Mount St. Elias region (Fig. 2), eastward approximately from Icy Bay, the fold-thrust belt becomes more complex through a combination of basement involved thrusting and 3D structural complications related to simultaneous strike slip and contractional deformation (Chapman et al., 2012). The coincidence between this structural transition, a change in basement type from a mafic crust to the west versus a more complex basement to the east, and the area of highest terrain in the orogen has long been recognized (e.g., Plafker, 1987). In Bruhn et al. (2004), this and other relationships were used to divide the orogen into three distinct segments (Fig. 2): (1) the Yakutat segment on the east, where basement-involved thrusts and the Fairweather strike-slip system represent a slip-partitioned, oblique-convergent dextral transpressional system; (2) the central Yakataga segment, which represents the main fold-thrust belt where the structure approaches plane-strain contraction; and (3) the western Katalla segment, which forms the western syntaxis of the orogen where early-formed fold-thrust structures are refolded into complex geometries. We consider the structure of the Yakataga segment and its transition into the Yakutat segment.

METHODS AND SCOPE OF THIS STUDY

In this paper, we summarize the results of three field seasons of geologic mapping in the Yakataga segment; the bulk of our work was concentrated along two transects (Fig. 2). The field work in 2005–2006 was supported primarily by helicopter placement of fly camps and mapping conducted on foot from these camps. In 2007, we completed the field effort through one week of helicopter-supported traverses and spot checks within the area shown in Plate 1, and five days in the Icy Bay region (Plate 2). The total field effort in person days includes ~100 in 2005, 60 in 2006, and 100 in 2007.

During the field effort, we used digital field mapping techniques based on the software package ArcPad using hand-held computers and camp-based tablet computers. The field methods for our approach were summarized in Pavlis et al. (2010). In addition to conventional mapping of lithostratigraphic units, we also systematically mapped the surface traces of bedding and foliation (Plates 1 and 2). This technique is well established in the structural analysis of metamorphic terranes, and the map of metamorphosed rocks in the high-altitude regions of the Icy Bay area (Plate 2) is a good illustration of the technique. In this study, the technique also proved valuable in unraveling the structural details in unmetamorphosed rocks because the formal rock units are too thick and too monotonous to resolve structures at scales >~1:100,000.

Field files were merged and refined in ArcGIS software following each field season, and these data were extended during each field season. Following the field effort, we produced preliminary digital geologic maps through merging our data with reconnaissance mapping by G. Plafker (both digital compilations in Wilson et al., 2005; Richter et al., 2006, and from copies of paper field sheets, G. Plafker, written communication to Pavlis and Bruhn, 1999) and Miller (1957, 1971) as well as our own mapping from the late 1990s. For the Duktoth River region (Fig. 2; Plate 1), we then overlaid these data onto georeferenced, high-resolution imagery that included ~2-m-resolution U2 aerial photography and a satellite image (~1 m resolution) that was obtained in 2008. This imagery was used to refine and extend the mapping. We used a similar approach for the Icy Bay region (Fig. 2), but had access to a higher resolution image (~0.5 m) for the eastern part of the mapped area and similar ~1-m-resolution imagery for the western part. However, this 0.5–1 m imagery was not obtained until late in the project (2010), and we have not been able to field check much of our image interpretation.

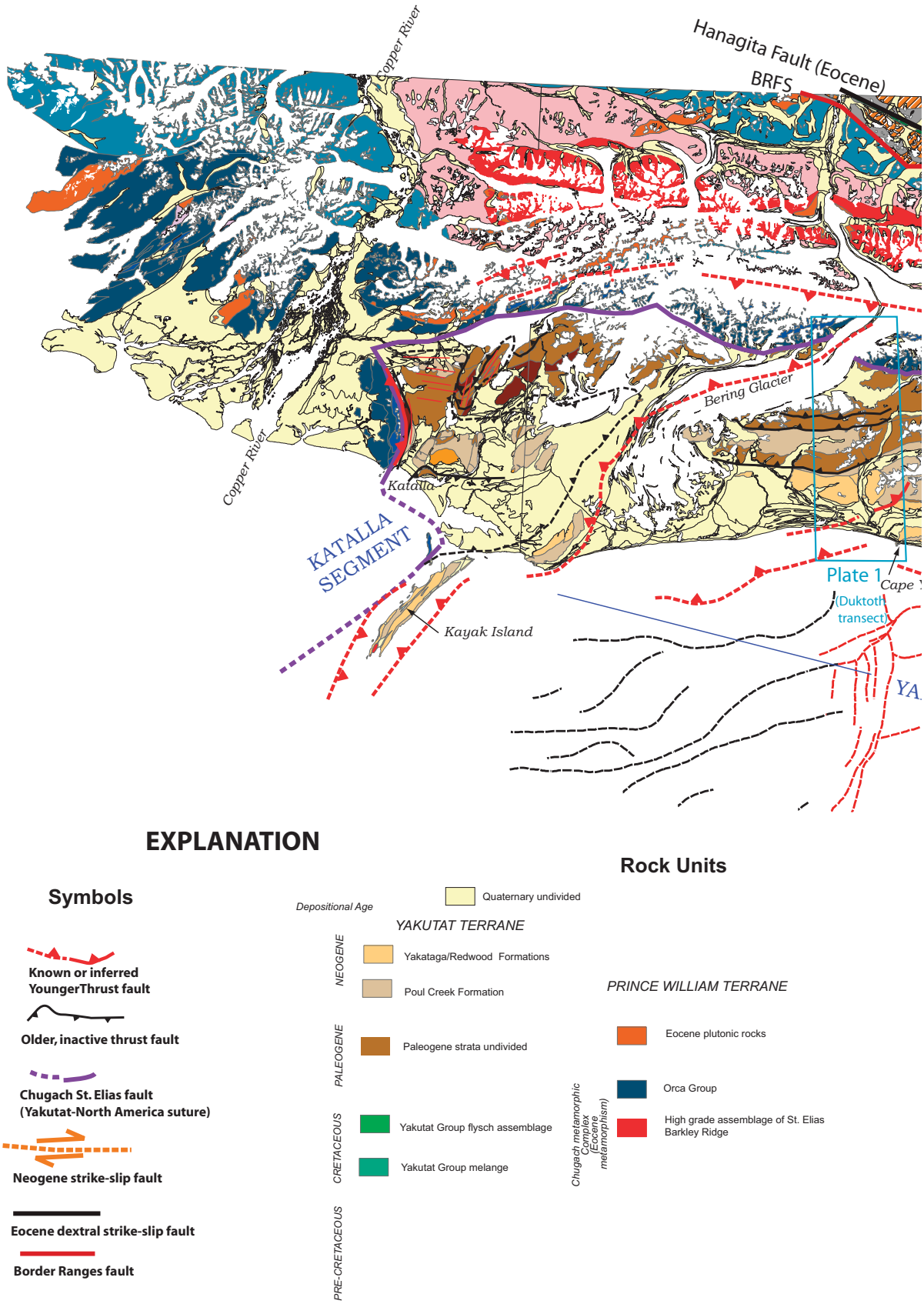

Figure 2 (*continued on following page*). Regional geologic map of the core of the St. Elias orogenic belt showing the locations of our detailed mapping and inferred active structures based on our work. Map was prepared from geographic information system (GIS) files of Wilson et al. (2005) and our digitization of the

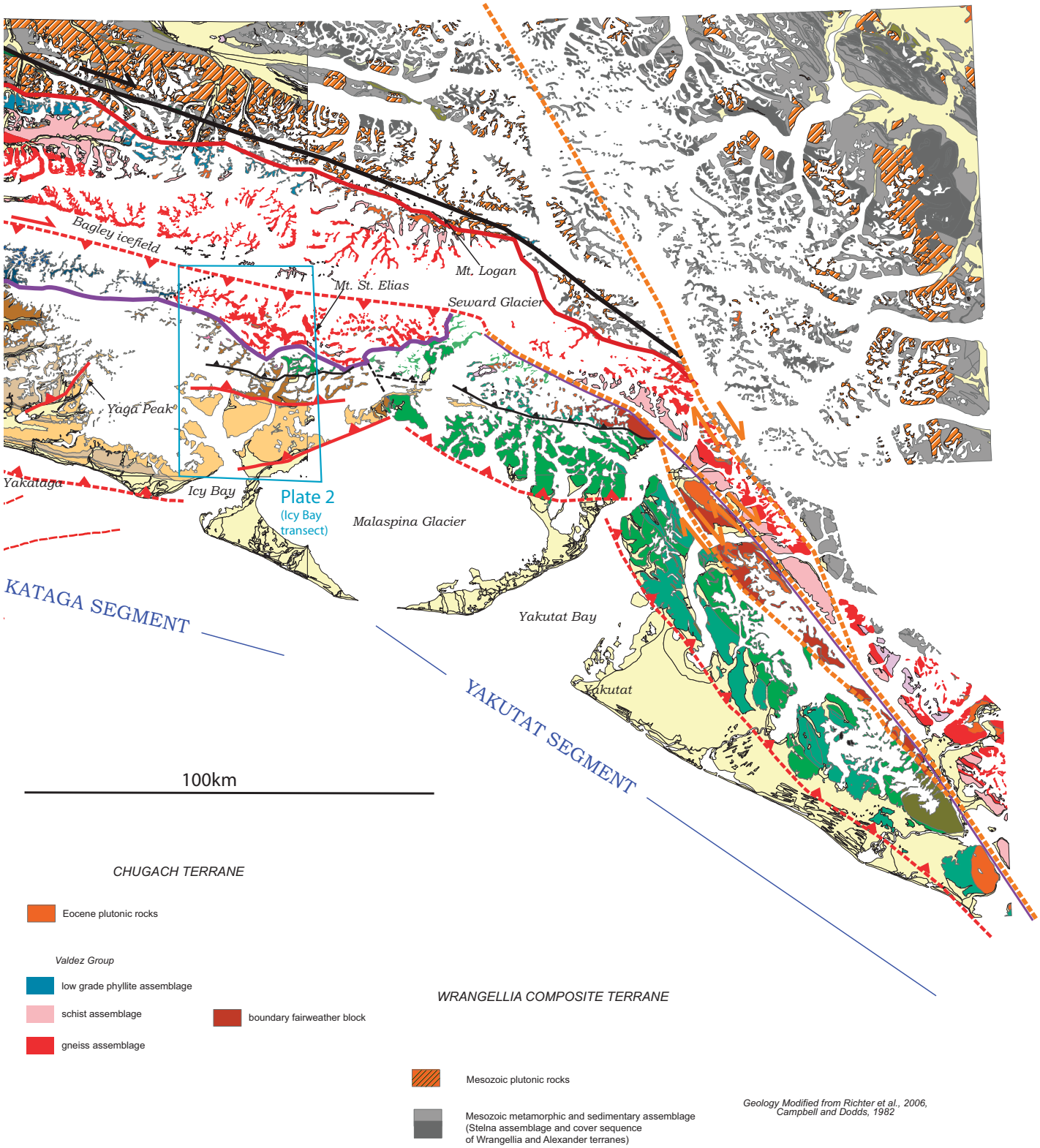

St. Elias region from mapping by Campbell and Dodds (1982). Note discrepancies between this map and our mapping (Plates 1 and 2) as well as mapping by Scharman et al. (2011) and Gasser et al. (2011) that have not been incorporated as modifications of the GIS files. BRFS—Border Ranges fault system.

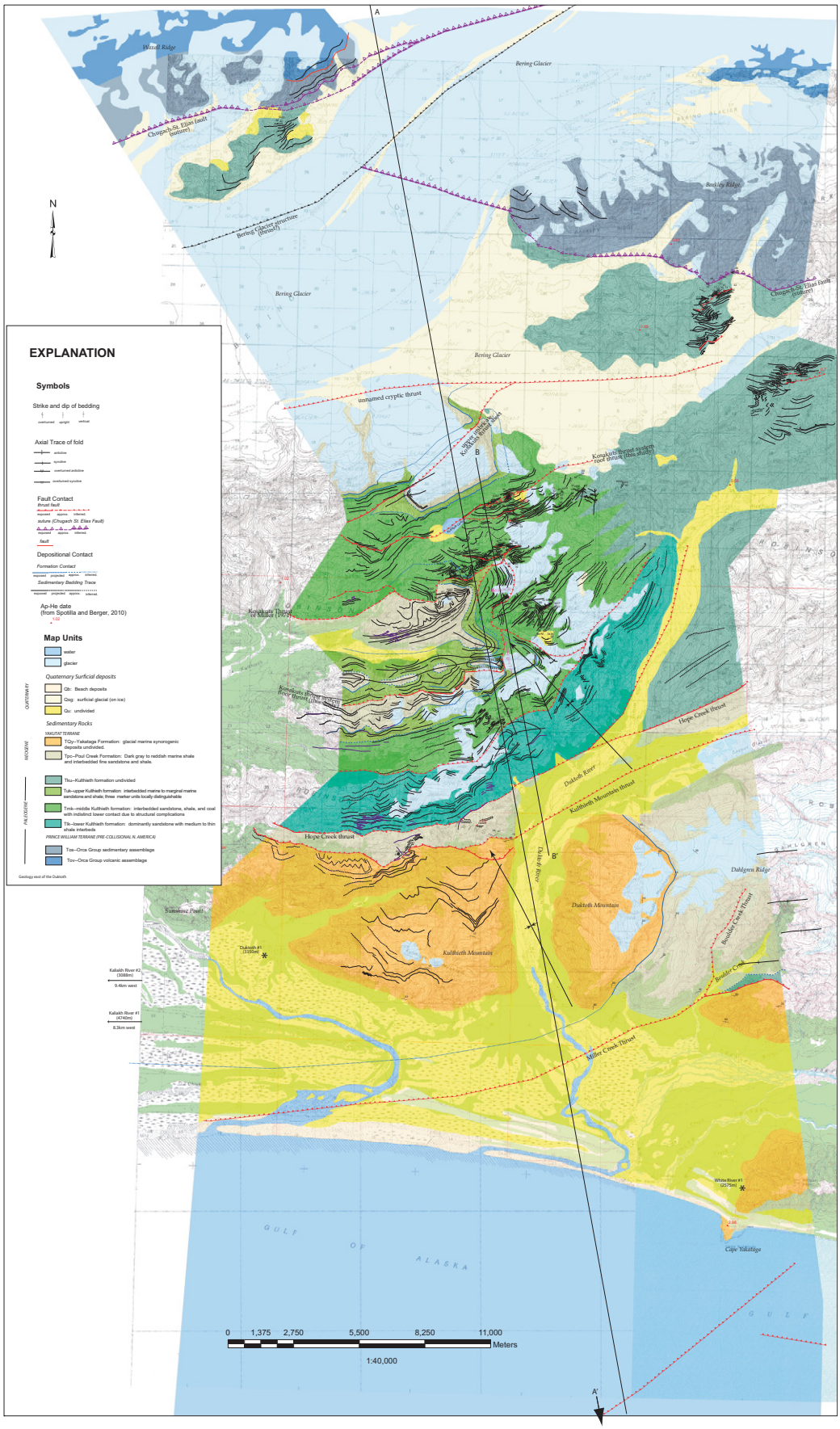

Plate 1. Geologic map of the Duktoth River transect. This figure should be viewed as an oversized figure at its full size of 88 × 150 cm. To print this figure, use a large format plotter at least 36″ (~91 cm) wide. To view Plate 1 online, please visit http://dx.doi.org/10.1130/GES00753.S4 or the full-text article on www.gsapubs.org.

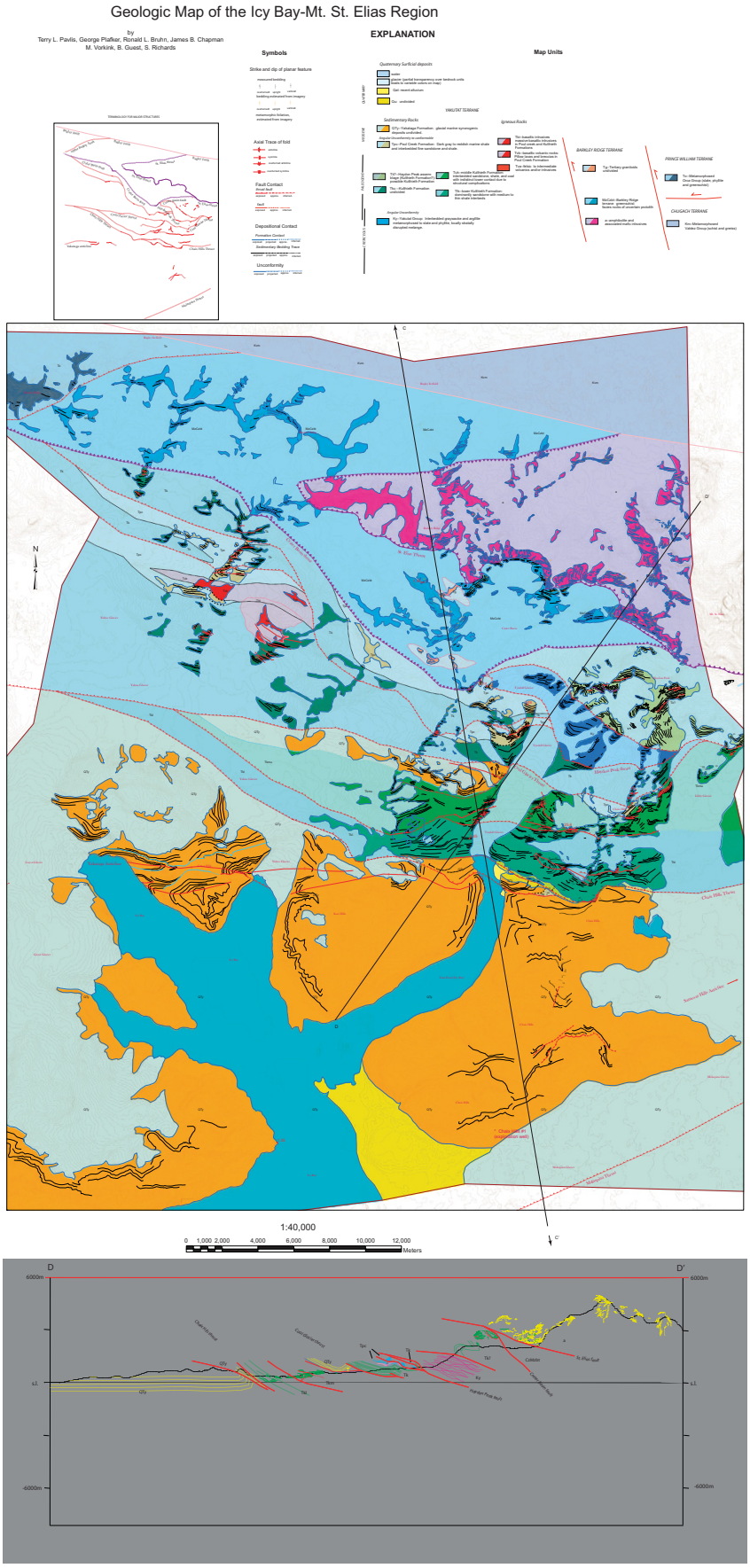

Plate 2. Geologic map of the Icy Bay transect with accompanying detailed cross section along Icy Bay. This figure should be viewed as an oversized figure at its full size of 107 x 183 cm (42 x 72 in). To print this figure, use a large format plotter at least 42″ (~107 cm) wide. To view Plate 2 online, please visit http://dx.doi.org/10.1130/GES00753.S5 or the full-text article on www.gsapubs.org.

Most of the interpretations of the higher elevation regions in the northern part of Plate 2 are based on these satellite images (see Supplemental File 1[1]).

Following completion of the mapping, we draped the 2D maps onto a 30 m digital elevation model (DEM). We worked with a regional, Advanced Spaceborne Thermal Emission Radiometer (ASTER) 30 m DEM because these data reflect modern deglaciated terrain and cover the entire region, whereas Shuttle Radar Topography Mission (SRTM) data are limited to latitude below 60.3°N. The accuracy of the ASTER DEM is uncertain; it does not correlate closely with existing topographic maps in some areas, particularly high-altitude, remote sites, and it is not clear which data are at fault. We suspect that the ASTER DEM is at fault because orthorectifying high-resolution images to this DEM produces significant pixel smear in areas that also show deviations from topographic maps. Future geodetic studies need to resolve the discrepancies in base maps in this region.

The 3D map data were then exported to the software package Move (Midland Valley Ltd.; http://www.mve.com/). We used three versions of Move (Move 2009, 2010, and 2011) with three modules within the software package: 2D move, which is largely used for cross-section construction; 3D move, which is used for 3D model generation and viewing; and 4DMove/Move, which merges the other two packages through visualization and data import-export function. This software allowed 3D visualization of the data reported here, and 2DMove was used for all cross-section construction and restorations reported herein. The bedding trace map developed during our field studies was particularly valuable when used with this software because the software contains map trace projection tools that allowed projection of our surface data onto cross-section views for further analysis. For example, the cross section included as part of Plate 2 contains virtually no interpretation other than line smoothing, and was generated by direct projection of line work from the 3D geologic map. In our cross-section restoration, we used Move's fault-parallel flow model for fault restorations and the trishear and flexural slip models to restore folds.

[1]Supplemental File 1. Zipped file containing final ArcGIS geodatabase for Plates 1 and 2. These files require ArcGIS v. 9 or 10 software or other GIS software that can read geodatabase files. The files contain the metadata for these files and further information on the data. If you are viewing the PDF of this paper or reading it offline, please visit http://dx.doi.org/10.1130/GES00753.S1 or the full-text article on www.gsapubs.org to view Supplemental File 1.

STRATIGRAPHY OF THE YAKATAGA SEGMENT

Plafker (1987) and Plafker et al. (1994) summarized the general stratigraphic framework of the Yakutat terrane, and STEEP work (Landis, 2007; Witmer, 2009) provided further information (Fig. 3). The stratigraphic units show significant differences between the Icy Bay and Duktoth River areas, and are summarized in the following, from oldest to youngest.

Kulthieth Formation

In the Yakataga segment, the Eocene Kulthieth Formation (Fig. 3) is the basal unit of the Yakutat cover sequence and is dominated by fluvial sandstone and shale with coal that transitions upward into overlying marine deposits of the Poul Creek Formation (Plafker, 1987; Landis, 2007). The base of the unit is only exposed just east of the Icy Bay transect in the Samovar Hills (Plafker, 1987; Landis, 2007; Chapman et al., 2012), where it overlies with angular unconformity both the accretionary complex basement (Yakutat Group) and complex clastic-volcanic units that include conglomerate, sandstone, siltstone, basaltic flows, and andesitic pyroclastic rocks (siltstone of Oily Lake and Hubb's Creek volcanics of Plafker, 1987). The top of the Kulthieth Formation is exposed in the Duktoth River transect, where it grades into the overlying Poul Creek Formation. In the Samovar Hills and the Icy Bay transect, however, the top of the Kulthieth Formation as well as overlying strata are cut out along an angular unconformity, with the Poul Creek Formation preserved only locally (Fig. 3). This upper angular unconformity can be traced westward from the Samovar Hills, where it cuts upsection and disappears

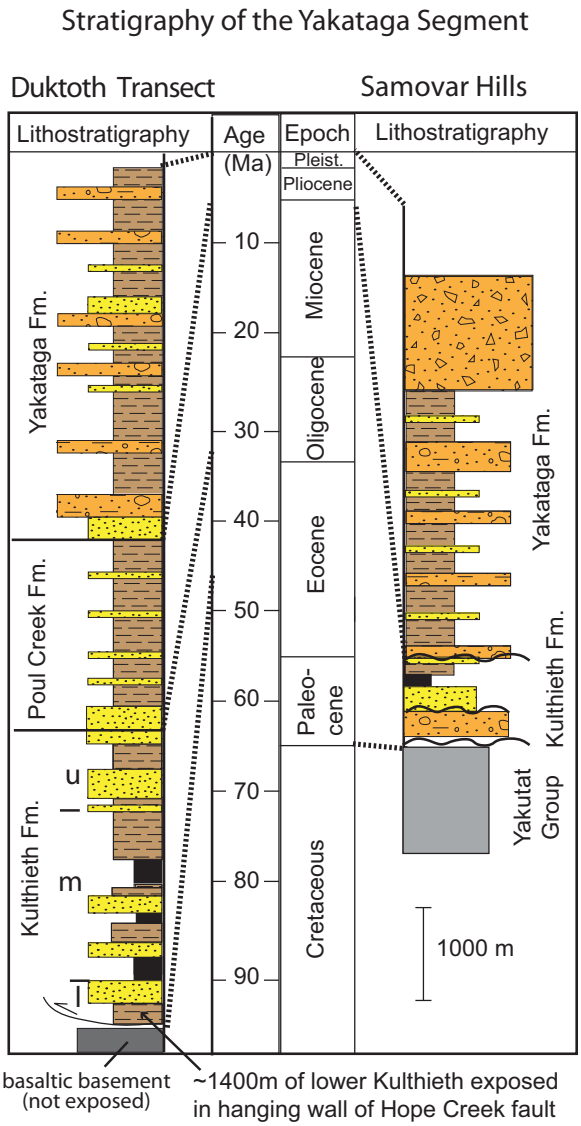

Figure 3. Generalized lithostratigraphy of the mapped areas in Plates 1 and 2. Crystalline rocks of the Mount St. Elias region are not included in this diagram. Pleist.—Pleistocene; u—upper; m—middle; l—lower.

beneath the icefields to the west (Fig. 3; Plate 2). The total thickness of the Kulthieth Formation is difficult to decipher, but a section measured by Landis (2007) in the Duktoth River area indicates that the unit is at least 2.8 km thick.

In both the Duktoth River and Icy Bay areas, the Kulthieth Formation can be subdivided into three general divisions (Fig. 3; Plate 1). From base to top these subunits include: (1) a lower member, composed of thick-bedded sandstone with broad lenticular geometries; (2) a middle, lithologically heterogeneous member, composed of 1–4 m interbeds of ripple-laminated siltstone, carbonaceous shale, micaceous sandstone, and coal; and (3) an upper member composed of interbedded shale, siltstone, and sandstone.

The precise contacts between the subunits are typically gradational, and structural complexity makes routine mapping of the contacts difficult. Although we show the approximate trace of the lower-middle Kulthieth contact on the geologic maps, we were not able to routinely map this contact in the field because (1) the contact is gradational, and probably even shows major changes in fluvial facies across the area, complicating recognition of a single stratigraphic horizon; and (2) the middle Kulthieth is characterized by complex trains of detachment folds that typically detach along coal horizons. These detachment surfaces further complicate recognition of a distinct stratigraphic horizon, but are the primary criteria used in mapping the lower-middle Kulthieth contact shown on our maps. This detachment horizon interpretation is highlighted through the mapping of the lower-middle Kulthieth contact as a thrust fault in both maps (Plates 1 and 2).

The middle to upper Kulthieth transition in the Duktoth River area represents the base of a nonmarine to marine transition with coal-bearing deltaic strata below and marine coastal sandstones and shales above (Landis, 2007). In our mapping, we were able to routinely map this transition as well as two marker beds within the upper Kulthieth throughout the Duktoth River area (shown as bedding traces on the geologic map; Plate 1).

Poul Creek Formation

The marine Poul Creek Formation depositionally overlies marine strata of the upper Kulthieth Formation. These rocks were deposited during a relatively long time interval, from Late Eocene to Early Miocene, and record moderate to deep-water deposition (Plafker, 1987). In the Icy Bay area, the Poul Creek Formation is largely removed by erosion along an angular unconformity (Fig. 3), but appears locally as fault slices and in the footwall of two of the thrust systems. In the Duktoth area, the Poul Creek is characterized by a lower, reddish-brown, dominantly fine sandstone and/or siltstone interval (~300–500 m thick) overlain by shale, siltstone, and fine sandstone that are rhythmically interbedded at scales of 10–30 cm. The lower Poul Creek unit is the equivalent of the Split Creek sandstone mapped to the west in the Katalla area (Miller, 1975). Although it may be possible to divide the Poul Creek Formation in this area, we were not able to routinely make this subdivision in our limited field time because the contact is gradational. Volcanic rocks are locally interbedded with the Poul Creek Formation elsewhere in the St. Elias orogen (Plafker, 1987). Poul Creek volcanic rocks and related intrusives are mapped in nunataks in the upper Yahtse Glacier and probable Poul Creek igneous rocks are inferred from photo interpretations of upper Icy Bay (Plate 2). The only igneous rocks observed in the Duktoth area are dike rocks.

Yakataga Formation

The youngest strata in the mapped areas comprise a complex package of fluvial and/or braid-delta and glaciomarine, synorogenic strata referred to collectively as the Yakataga Formation. The Yakataga Formation ranges from absent to at least 5 km in thickness; it contains intraformational, commonly angular, unconformities associated with fold growth, and ranges in age from Late Miocene to recent (Plafker, 1987; Lagoe et al., 1993; Arnaud, 2010). In line with previous workers, we were unable to subdivide the Yakataga Formation beyond construction of bedding form lines to constrain the structure. The unit includes a great variety of sedimentary lithologies, ranging from dark mud and/or mudstone to boulder, matrix-supported conglomerate. However, the rocks are characterized mainly by sandstone and diamictite; along with presence of abundant marine fossils, this represents the primary basis for their interpretation as glaciomarine strata (Plafker and Addicott, 1976; Eyles et al., 1991; Witmer, 2009).

Onshore, the Yakataga Formation occurs only in the two outermost thrust sheets in both mapped areas (Plates 1 and 2). These strata continue offshore, where they are well imaged in seismic data and include sediments as young as late Pleistocene and Holocene. These rocks were recognized in drill cores from seven exploration wells in this area: Chaix Hills Well #1, Chaix Hills Well #1A, and Rioux Bay in the Icy Bay area (Plate 2), and Duktoth #1, Kaliakh River #1, Kaliakh River #2, and White River #1 in the Dukoth River area (Plate 1). We examined cores from five of these wells (Chaix Hills, Kaliakh River, and Duktoth #1) at the State of Alaska archive. The amount of core is very limited in the archive, particularly the Kaliakh and Duktoth wells, but we observed only Yakataga Formation in the available material. Plafker (1967, 1971) reported the Poul Creek(?) Formation in the Kaliakh wells and the Duktoth #1 well, and given the limited archive we probably did not see these Poul Creek samples. Moreover, lithologic logs are consistent with Poul Creek in these wells. Nonetheless, because of the conspicuous structural complications in these cores (e.g., high bed dips in many) it is difficult to use Poul Creek Formation tops to estimate stratigraphic thicknesses for the Yakataga Formation from these wells. In the Icy Bay area, Plafker (1967) reported the Poul Creek Formation in the Rioux Bay well, and because bedding in this region is relatively flat lying, the occurrence of the Poul Creek Formation in the well can be used to estimate a total Yakataga thickness of ~4 km in this area.

GEOLOGIC STRUCTURE OF THE YAKATAGA SEGMENT

Duktoth River Transect

A focus of the STEEP field efforts was the development of a well-constrained cross section through the Robinson Mountains just west of the Duktoth River (Fig. 2; Plate 1). The structure within this transect is now reasonably well determined such that our final geologic map (Plate 1) is accurate to a nominal scale of ~1:25,000. Significant data gaps exist along the northern 20%–25% of the transect due to extensive cover by a large tributary of the Bering Glacier. To minimize this problem, our mapping includes structures along the ridge at the head of this glacier, up to the trace of the Chugach–St. Elias fault.

The general structure recognized in our mapping is consistent with the original reconnaissance work of Miller (1957, 1971), Plafker (1987), and Richter et al. (2006), but structural details recognized during our work provide important new constraints on the structural evolution of this transect. In line with previous studies, we recognize four major exposed thrusts, and infer a fifth thrust beneath ice cover. These include, from south to north (Plate 1): (1) the Miller Creek fault; (2) the Hope Creek fault and an associated slice of Poul Creek Formation above the Kulthieth Mountain fault; (3) the Kosakuts thrust, which comprises a complex thrust stack within the transect (Fig. 4); (4) an inferred thrust that places the Kulthieth Formation onto the Poul Creek Formation beneath the Bering Glacier; and (5) the Chugach–St. Elias fault. Following Bruhn et al. (2004, 2010), we also infer

a young sixth thrust beneath the Bering Glacier to account for mismatches of the Chugach–St. Elias fault across the glacier (Plate 1) and other evidence for a structure along this glacial valley (Bruhn et al., 2010). Structures associated with the entire thrust complex become increasingly complex from south to north.

Miller Creek Thrust Sheet

The lowermost exposed thrust sheet in the mapped area (Plate 1) comprises the hanging wall of the Miller Creek fault of Miller (1971). This fault is not exposed west of the Duktoth River (Plate 1), but is recognized in the subsurface in wells. Our analysis of cores from these wells indicates that the footwall of the Miller Creek fault contains at least 3000–4000 m of Yakataga Formation (Kaliakh #1 and Duktoth #1 wells; Plate 1).

From Sunshine Point eastward to the Duktoth River, the Miller Creek thrust sheet is a deceptively simple north-dipping homocline in the Yakataga Formation (Plate 1). Analysis of Miller's (1957, 1971) mapping to the east of the Duktoth River, however, reveals a much more complex structure within this thrust sheet.

From Duktoth Mountain eastward along Dahlgren Ridge, the structure of the Miller Creek thrust sheet shows complications indicating 3D deformation, which we interpret as a result of structural overprints during progressive deformation. Meigs et al. (2008) interpreted the Miller Creek fault in this area as an out-of-sequence thrust because of structural details near the Yakataga Glacier, and our analyses support this conclusion. However, we extend the Meigs et al. (2008) interpretation to infer a pair of northeast-striking thrusts that are oblique to, and younger than, the primary trace of the Miller Creek fault to account for the 3D structural complexity in this area. The best constrained of these inferred structures is referred to here as the Boulder Creek thrust (Fig. 2; Plate 1), named for its inferred trace subparallel to Boulder Creek. Although not directly mapped by Miller (1957), we infer this thrust based on three lines of evidence.

1. To the west of Boulder Creek (Plate 1), bedding in the Poul Creek Formation is concordant to the moderately west dipping bedding in the overlying Yakataga Formation, indicating a thick homoclinal section. Just to the east of Boulder Creek, however, the Poul Creek Formation is folded into a series of short-wavelength, approximately east-west–trending, upright horizontal folds. This structural discordance requires, at the least, a detachment surface between the homocline and the folded sections, but a simpler explanation is a northwest-dipping thrust between these structural domains.

2. East of Boulder Creek, the trace of the Miller Creek thrust is consistent with a relatively planar, east-west–striking, moderately north dipping thrust extending approximately parallel to bedding in the upper Kulthieth Formation, just below the Poul Creek contact. However, if the fault continued westward as a planar structure, the fault would continue across Boulder Creek at this stratigraphic level. Instead, northwest-dipping Poul Creek formation occupies the west bank of Boulder Creek (Plate 1); this geometry could result from simple, convex-upward curvature of the Miller Creek fault. Nonetheless, if this were true, the fault should cut downsection toward the west, bringing Kulthieth Formation to the surface west of Boulder Creek; this is inconsistent with the mapped geometry. More complex geometries with lateral ramps or thrust branch lines are certainly allowable, but the simplest interpretation of this map pattern is that a northeast-striking, younger fault, the Boulder Creek thrust, cuts the original approximately east-west–striking Miller Creek fault.

3. The west-dipping section on Duktoth Mountain displays bedding strikes nearly perpendicular to the regional approximately east-west strikes and north dip of ~20° just across the Duktoth River at Kulthieth Mountain (Plate 1). This observation, together with the absence of angular unconformity at the Yakataga–Poul Creek contact, implies that the Duktoth Mountain section was tilted westward as a unit. This tilt sense is consistent with a west- or northwest-dipping listric thrust along Boulder Creek producing a hanging-wall syncline.

Farther east, we infer a second, northeast-trending younger thrust just west of Yaga Peak (Fig. 2). This structure is more speculative than the Boulder Creek thrust, but is suggested by: (1) an abrupt change in bedding strike and dip along the inferred trace of the fault, and (2) a distinct structural high to the west (Dahlgren Ridge anticlinorium of Wallace, 2008) with approximately east-west–trending structures that are oblique to a long-wavelength, open, northeast-trending footwall syncline (Yaga syncline) immediately to the east developed in a thick section of Yakataga Formation.

We recognize that there are alternative explanations for the structural geometry of the Miller Creek fault. For example, blind structures beneath the Dahlgren anticlinorium of Wallace (2008) could produce structural relief and secondary folding resulting in some of these features. Nonetheless, in the absence of other data, the simplest interpretation is that the Miller Creek thrust sheet has been cut by younger northwest-dipping thrusts that disrupted the general east-west trends within intervening segments of the thrust sheet. We infer that the general west dips of the Poul Creek and Yakataga strata at Duktoth Mountain are direct results of this structural superposition and, together with the Kulthieth Mountain homocline, the strata form a broad, north-northwest–trending syncline (Plate 1) that is oriented at nearly right angles to the regional structural trends. This general structural style is reminiscent of, but less complex than, the two-phase folding of Tertiary strata immediately to the west in the Katalla segment of the orogen (Bruhn et al., 2004). We interpret these structures very differently, however, and tie the younger structures to erosion and tectonic interactions within the orogenic wedge (see following).

Hope Creek Thrust Sheet

The Hope Creek thrust sheet shows the largest stratigraphic throw in the Duktoth transect, other than the Chugach–St. Elias fault suture, and our mapping is consistent with the Meigs et al. (2008) interpretation that the Hope Creek fault is a major thrust. The fault system is composed of two distinct strands (Plate 1): (1) a lower thrust, the Kulthieth Mountain thrust of G. Plafker (1999, written communs.) that places the Poul Creek Formation onto the Yakataga Formation; and (2) an upper thrust that places the lower Kulthieth Formation onto the Poul Creek Formation. The upper fault appears to be the more significant fault of the pair because it is bedding parallel in both the hanging wall and footwall, implying a thrust flat on thrust flat relationship. In contrast, the lower thrust places the Poul Creek Formation with an anticlinal rollover on top of the Yakataga Formation, with bedding dipping less than the fault; this relationship indicates a footwall cutoff and a hanging-wall cutoff with an associated anticline. This geometry along the lower thrust, together with the basic map pattern, suggests strongly that the lower thrust represents the base of a large Poul Creek horse caught up along the thrust, and this horse is along a footwall cutoff in the Yakataga Formation (Plate 1 and Fig. 6).

The hanging wall of the Hope Creek thrust varies in structural complexity with structural level within the thrust sheet. The lower ~1 km of the thrust sheet is broadly homoclinal, with lower Kulthieth Formation dipping parallel to the underlying thrust (Plate 1 and Fig. 6). Above this stratigraphic level, however, is a band of moderately to tightly folded middle Kulthieth Formation, which passes up structural section into a second, north-dipping homoclinal domain composed of upper Kulthieth Formation and the lowermost part of the Poul Creek Formation. The details of the complex fold structures in the middle part of the thrust sheet are not well understood, but these folds probably represent a detachment fold duplex developed within the

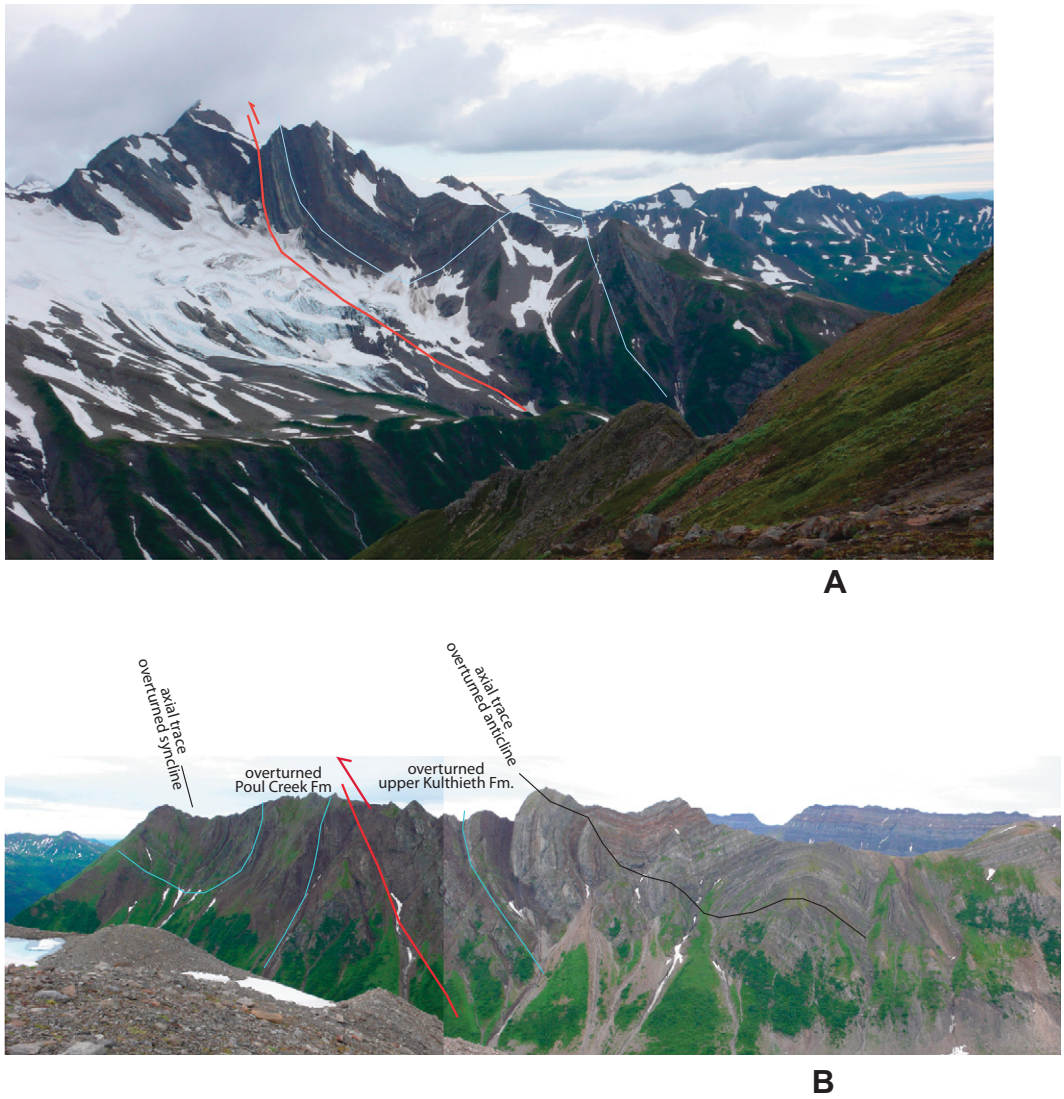

Figure 4. Field photographs of structural relationships in the Kosakuts thrust sheet that can be compared to the detailed cross section in Figure 6. (A) View toward the west of the leading thrust of the Kosakuts sheet. Note the footwall cut-off and hanging-wall flat and the conspicuous hanging-wall folds. (B) Photo mosaic view of the complex folding and faulting in the overturned limb of the large synclinorium within the thrust sheet. Note the conspicuous anticline above the minor thrust indicated by the line along the axial trace.

coal-bearing middle Kulthieth Formation. In our cross sections (Fig. 6), we have simplified this structure as a pair of bedding-parallel faults bounding the middle Kulthieth Formation, but the actual structure is undoubtedly much more complex.

The Hope Creek thrust sheet displays 3D complexities similar to those of the Miller Creek thrust sheet, but is more subtle because the structures are entirely within the Kulthieth Formation. Most notable is a broad, systematic change in bedding orientations from approximately north dips in the western half of the area to northwest dips along the Duktoth River to the east. This pattern is most prominent in the lower part of the thrust sheet where smaller scale folding is not significant, but it is also recognizable at higher structural levels. This spatial pattern suggests a broad, northwest-plunging synclinorium (Plate 1) similar to the structure of the Miller Creek thrust sheet, a geometry consistent with stereonet plots for bedding-plane measurements within the thrust sheet (Fig. 5).

Kosakuts Thrust Sheet

Miller (1971) and Plafker (*in* Richter et al., 2006) mapped a regional thrust separating a northern belt of Kulthieth Formation from a synclinorium at the top of the Hope Creek thrust sheet and referred to this structure as the Kosakuts thrust. Our observations support the existence of this thrust, but the new mapping demonstrates that this thrust sheet is a complex fold-thrust stack that involves imbrication of the middle and upper Kulthieth Formation as well as the Poul Creek Formation. As a result, our mapping places the leading thrust of this imbricated sequence to the south of the map trace shown on regional maps and a trailing thrust well to the north (Fig. 2; Plate 1).

The leading thrust of the Kosakuts thrust sheet is spectacularly exposed on a north-northwest–trending ridge near the center of the mapped area (north of peak 4463, near Universal Transverse Mercator [UTM] 410900,6682500, z7 NAD83 [North American datum]), where the thrust places the upper Kulthieth Formation on top of the Poul Creek Formation (Fig. 4A; Plate 1). This thrust is difficult to trace eastward beyond this ridge because it places middle Kulthieth Formation on top of upper Kulthieth Formation, and our field observations are too widely spaced to unequivocally trace the thrust. Nonetheless, we infer that the thrust cuts parallel to bedding through a largely homoclinal section, forming a floor to the thrust complex (Plate 1 and Fig. 6).

Structurally above this leading thrust is a fold-thrust complex developed within the middle Kulthieth to Poul Creek Formations. The most prominent feature within this complex

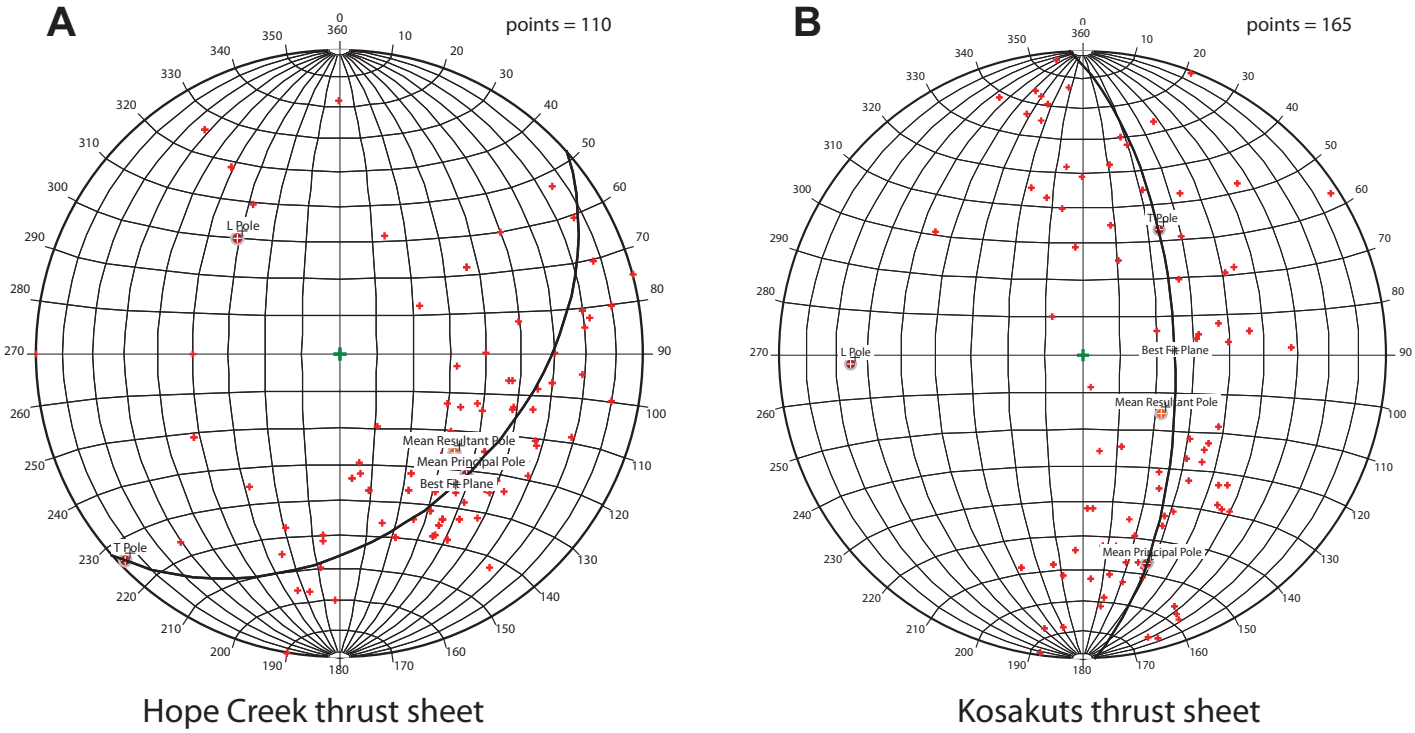

Figure 5. Equal-area, lower hemisphere stereographic projections of poles to bedding in two structural domains within the Duktoth map area. (A) Hope Creek thrust sheet. Bedding planes from the relatively homoclinal domains of the lower Kulthieth Formation, illustrating the open, northwest-plunging fold system that is superimposed on older structure. (B) Bedding orientations from the large fold complex within the Kosakuts thrust sheet, showing the west plunge of these major fold systems.

is an overturned, steeply inclined, gently west-plunging anticline-syncline pair that is faulted complexly on the overturned limb (Plate 1; Figs. 4B and 6). Bedding-plane measurements from within this fold complex confirm the general west plunge of this fold complex (Fig. 5). The fold system has a wavelength of ~3 km, but contains numerous secondary folds, particularly in the Kulthieth Formation. This fold pair is in turn structurally overlain by at least three smaller scale thrusts that duplicate the Kulthieth Formation, which is complexly folded within each imbricate (Figs. 4B and 6). This fold-thrust complex is structurally overlain by a thick homoclinal panel of middle Kulthieth Formation to Poul Creek Formation that contains one minor fold-thrust imbricate within the structural section (labeled as upper imbricate of Kosakuts thrust sheet; Plate 1).

This general structural succession suggests that the Kosakuts thrust sheet is a composite thrust system with internal imbrication and folding (Fig. 6). A detailed section (Fig. 6) and field views (Fig. 4) show numerous structural complexities, particularly fold systems that are characterized by parallel-fold layers of sandstone interlayered with coal and shale layers that accommodate folding by flow to produce variable thickening in fold hinges. Although complex, the general structural succession suggests that the Kosakuts thrust sheet cannot be ascribed solely to simple fault-bend folding or detachment folding. Instead, we suggest that the basic structure is dominated by the development of an antiformal stack with extensive folding within thrust slices accommodated by flexural flow. In this interpretation, the structurally highest thrust that passes beneath Kulthieth Lake (Plate 1) is a roof thrust to the antiformal stack duplex and the thrust below the fold-complex shown in Figure 4A is the floor. In addition, the Kosakuts thrust of Miller (1971) becomes a minor thrust within the antiformal stack, even though it is a prominent lithologic contact between the Kulthieth Formation and Poul Creek Formation.

The Kosakuts thrust sheet shows 3D complications closely linked to the structure of the underlying Hope Creek thrust sheet. In the central part of the mapped area (Plate 1), for example, the main syncline is a relatively simple fold in the upper Kulthieth and Poul Creek Formations, but to the east, the syncline is cut out by a fold-thrust complex in the Kulthieth Formation. Similarly, in the main ridge where the fold pair is well exposed, the folds have a shallow west plunge, but to the east bedding strikes turn to the northeast in association with the regional bedding changes recognized in the Hope Creek thrust sheet (Fig. 5). Collectively these observations suggest that the leading fold-thrust complex of the Kosakuts thrust sheet has been removed by erosion toward the east, presumably due to uplift driven by younger west tilts that formed the northwest-trending fold in the underlying Hope Creek thrust sheet.

Upper Thrust Sheet

At the top of the structural stack is the least well understood structure within the sequence (labeled unnamed cryptic thrust; Plate 1). We infer the existence of this thrust beneath the eastern arm of the Bering Glacier because a homoclinal panel of the Poul Creek Formation dips beneath the glacier, but on the north side of the glacier highly folded middle(?) Kulthieth strata indicate a stratigraphic reversal that is most easily explained by a major thrust along the glacial valley. At the eastern end of this valley, the Poul Creek Formation is absent and the thrust is unrecognizable where it duplicates only complexly folded middle Kulthieth strata. This suggests that the fault loses slip eastward as fold complexes within the middle Kulthieth Formation.

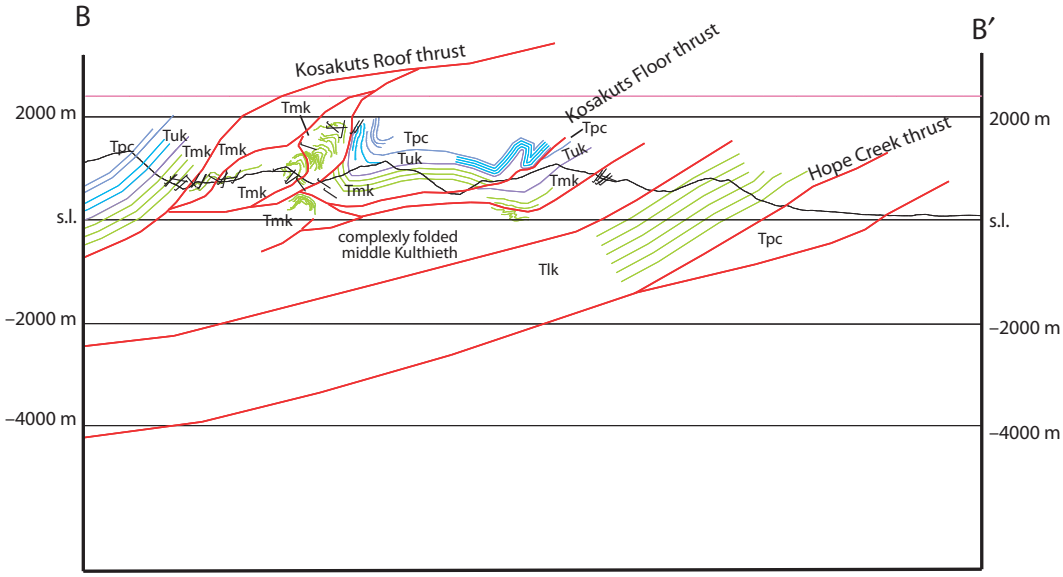

Figure 6. Detailed cross section across the Kosakuts and Hope Creek thrust systems with minimal interpretation. Most of this figure was prepared from projecting surface bedding traces onto the section line, and then simplifying the diagram for clarity. Note the complex structure of the Kosakuts thrust duplex. Tpc—Poul Creek Formation, Tuk—Upper Kulthieth Formation, Tmk—middle Kulthieth Formation, Tlk—lower Kulthieth Formation, s.l.—sea level. See Plate 1 for location of section.

The internal structure of the upper thrust sheet is not well understood. Where we have mapped these rocks, the entire section is characterized by complex, detachment-style folds with wavelengths from tens to hundreds of meters. This structural style is typical of middle Kulthieth coal-bearing strata throughout the mapped area, but incomplete exposure makes it difficult to generalize the structure within this part of the transect.

Synthesis—3D Structure

To illustrate our interpretation of this 3D geometry, we constructed simplified visualizations of key structures in the transect (Fig. 7; Supplemental File 2[2]). In this visualization, our subsurface control is poor, and is only meant to illustrate the basic structural association between the inferred northwest-dipping, out-of-sequence thrusts and the northwest-plunging open synclines in the hanging walls of the Miller Creek and Hope Creek thrust sheets. The key feature in this visualization is that motion on curved thrusts of approximately this geometry can account for the open, northwest-trending hanging-wall synclines as ramp synclines, although the slip vector for these faults would have to be more westward than the northwest-plunging hinge line of the synforms.

[2]Supplemental File 2. Move file (.mve) that was used to generate the static image in Figure 7 and contains a 3D representation of Plate 1 together with the section in Figure 10. Note that colors are changed in the .mve file for better clarity: pale blue is projected top of basement, red is the décollement, gray surfaces are known or inferred young faults within the system, dark blue is the base of the Yakataga Formation, and green is the middle-lower Kulthieth contact in the hanging wall of the Hope Creek thrust sheet. Readers can interact with this visualization by downloading the free viewer from Midland Valley at http://www.mve.com/resources/downloads. Note that this viewer requires either Microsoft Windows or Linux operating systems. If you are viewing the PDF of this paper or reading it offline, please visit http://dx.doi.org/10.1130/GES00753.S2 or the full-text article on www.gsapubs.org to view Supplemental File 2.

Icy Bay Transect

The general geology of the Samovar Hills region, including the Icy Bay area, was reported in Chapman et al. (2012). Here, we increase the scope of that effort through improved control on surface geology that was made possible through acquisition of new 0.5- and 1-m-resolution satellite images, and expand the geologic mapping westward into the upper Yahtse Glacier (Plate 2). The geology of the upper Yahtse Glacier is based on satellite image interpretation guided by the reconnaissance mapping of Richter et al. (2006) and Wilson et al. (2005) and 1:63,360-scale field maps from G. Plafker (1999, written commun.). The final result is a geologic map with an accompanying detailed cross section along the Tyndall Glacier (Plate 2).

The northern part of this area is very remote and we have only a few field observations from areas above ~1500 m elevation. Because of correlation ambiguities and confusion in terminology, we propose a new nomenclature for fault systems in this area to avoid future confusion (see inset, Plate 2) but suggest that this terminology should change when rock unit correlations are clarified.

Using this fault nomenclature (inset, Plate 2), we describe five major thrust sheets with several significant thrust systems within the individual thrust sheets. Several correlations in Plate 2 are suspect, but can be evaluated in future studies. We describe these thrust systems from structurally lowest to structurally highest in the following.

Malaspina Thrust Sheet

The leading, structurally lowest thrust is active, based on observations from the 1979 St. Elias earthquake (e.g., Estabrook et al., 1992) and from global positioning system (GPS) observations (Freymueller et al., 2008; Elliott et al., 2010; Elliott, 2011). Bruns and Schwab (1983) referred to this leading thrust as the Malaspina fault. This fault is not exposed at the surface and is presumed to reach the surface beneath the Malaspina Glacier. The thrust was apparently penetrated by the Chaix Hills #1 exploration well; dipmeter changes at depths of ~2500–2700 m suggest 2 distinct thrust faults in this interval. Moreover, our analysis of core from this well confirms the existence of slickensided fault rocks at the site of the upper dipmeter change, consistent with a thrust at this level rather than an angular unconformity (Fig. 11). Our inspection of well cores also indicates that the thrust duplicates only the Yakataga Formation at the well site, consistent with previous interpretations by Martin (1992) and Plafker et al. (1975). However, Plafker (1967) and Plafker et al. (1975) reported the Poul Creek Formation in Chaix Hills #1A, located only a few hundred meters south of Chaix Hills #1. We had no logs from Chaix Hills #1A and the amount of archived material is not large from this well, but unequivocal Yakataga conglomerates occur as little as 100 m above the upper thrust (depth of 8124 ft; 2476.19 m) and

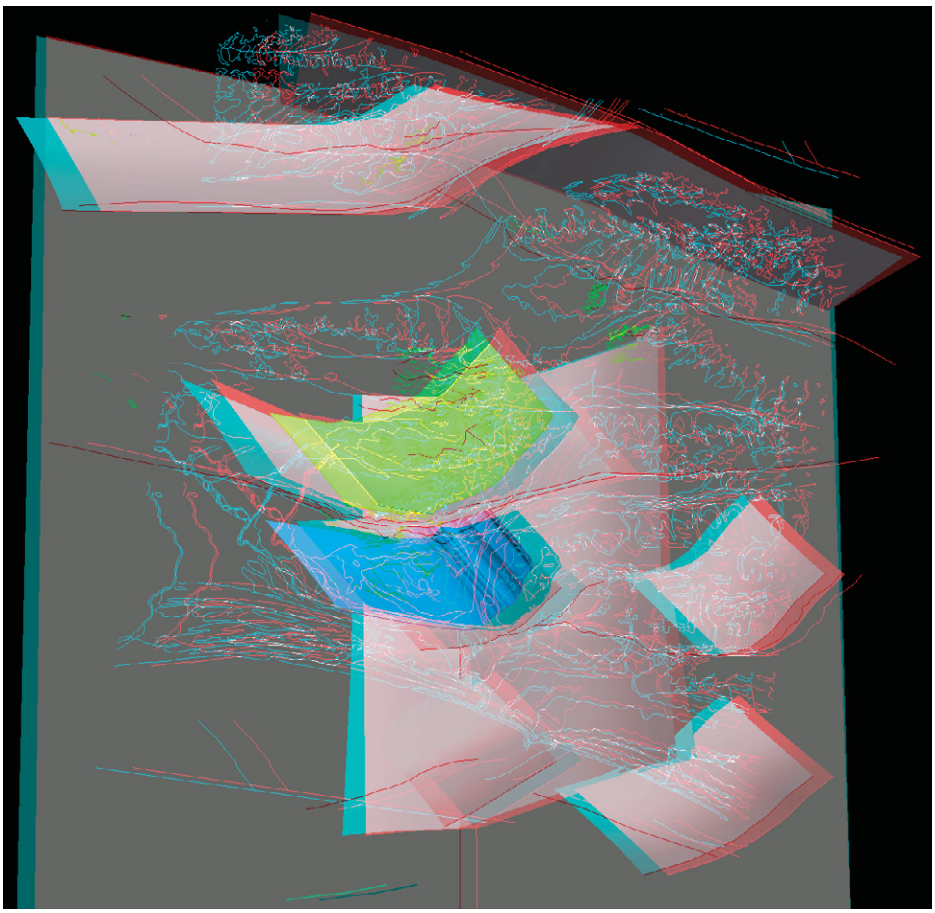

Figure 7. Three-dimensional (3D) visualization of the Duktoth River transect (geologic map from Plate 1). Static magenta-cyan stereo view shows the inferred 3D geometry of major young thrust systems as well as the geometry of two reference horizons that are warped into northwest-trending synforms associated with these younger faults. Light green—surface in the lower Kulthieth Formation above the Hope Creek fault; pale blue—basal Yakataga unconformity in the Miller Creek thrust sheet. See Supplemental File 2 (see footnote 2) for the Move file that was used to generate the static image seen here.

Yakataga conglomerates are abundant below the thrusts. Thus, if the Poul Creek Formation is present, it is only the uppermost Poul Creek. These observations provide important constraints on cross sections through this region, and although we assume that only the Yakataga Formation is in the well, a thin layer of uppermost Poul Creek would not alter significantly our subsurface interpretation (see following).

In the Chaix Hills, the Malaspina thrust sheet is internally imbricated by at least one minor thrust, but is structurally simple with homoclinal, gently north dipping strata (Plate 2). This simple structure is deceptive, however, because these homoclinal strata are along strike from the Samovar Hills anticline to the east and the Yakataga anticline to the west (Plate 2). In the Samovar Hills, an angular unconformity between simply folded Yakataga Formation strata and the underlying, complexly folded Kulthieth Formation records a complex history in that area (e.g., Plafker, 1987; Chapman et al., 2012). Similarly, the Yakataga anticline to the west is an anticline-syncline fold pair with spectacular Yakataga growth strata along the fold limbs (Broadwell, 2001). Broadwell (2001) interpreted this fold pair as a detachment fold with a blind thrust partially exposed in the fold core, and our mapping from high-resolution satellite imagery is consistent with that interpretation (Plate 2). In Chapman et al. (2012), the homoclinal section in the Chaix Hills was interpreted as younger growth strata at the lateral tip of the Samovar anticline; we add that these rocks are probably also growth strata on the lateral tip of the Yakataga anticline. This interpretation suggests that the Yakataga Formation above the Malaspina fault in the Chaix Hills represents a syntectonic basin between these two fold systems.

Chaix Hills Thrust Sheet

The Malaspina thrust sheet is structurally overlain by a major thrust that Plafker and Miller (1957) referred to as the Chaix Hills thrust. This fault places the lower Kulthieth Formation on top of the Yakataga Formation, a stratigraphic throw of ~6–8 km. The fault probably continues eastward as the Dome Pass fault (Chapman et al., 2012), but its continuation to the west is uncertain due to the extensive ice cover of the Yahtse Glacier (Plate 2). The thrust also carries a large slice composed of the upper Poul Creek Formation and lower Yakataga Formation with excellent exposure of the fault contact along Taan Fiord, and a small slice composed of Tertiary volcanic rocks (Poul Creek Formation volcanics?) in the Chaix Hills (Plate 2). The Chaix Hills fault is bedding parallel in the hanging wall, but shows a footwall cutoff in the Chaix Hills. The top of the Chaix Hills thrust sheet is marked by a thrust that is coincident in part with Plafker's (1967) Coal Glacier thrust, and we continue that terminology here (Plate 2). The internal structure of the Chaix Hills thrust sheet is complex, however, and includes complications by out-of-sequence thrusts and an angular unconformity near the top of the thrust sheet.

Immediately above the Chaix Hills thrust, the rocks are a relatively homoclinal, ~1-km-thick section that we correlate to the lower Kulthieth Formation. This homoclinal section appears to be continuous across the Taan Fiord and Tyndall Glacier valley; the only significant complication is along the ridge east of Taan Fiord, where the lower Kulthieth is repeated along a minor thrust that displays a lateral termination westward into an anticline-syncline pair (Plate 2).

Above this homoclinal section, middle Kulthieth coal-bearing strata are exposed; as in the Duktoth area, these rocks are folded complexly and imbricated at scales of tens to hundreds of meters. We infer a detachment surface in shales and coals at the structural transition from highly folded rocks to the lower Kulthieth homoclinal sequence. This surface is easily mapped on satellite imagery for this area, and the trace shown in Plate 2 is accurate in most areas to within a few meters to tens of meters where rock is exposed.

The internal structure in the upper part of the Chaix Hills thrust sheet is not well resolved due to structural-stratigraphic relationships that vary along strike as well as extensive ice cover obscuring details. Thus, there are alternative interpretations of structural geometry. Most significant among these complexities are marked variations across the Tyndall Glacier (Plate 2). Key observations include the following.

1. To the west of the Tyndall Glacier, the top of the thrust sheet is composed of a thick section

of the Yakataga Formation that is deformed into an open, upright, gently west plunging syncline. More significant, however, are observations demonstrating that this section of the Yakataga Formation was deposited above an angular unconformity with highly folded middle Kulthieth strata below (Chapman et al., 2012). Thus, a significant amount of the folding in the middle Kulthieth is relatively old, at least older than the latest motion on the Coal Glacier thrust that produced the footwall syncline. This observation is important because it demonstrates significant out-of-sequence thrusting within this transect and that this relative chronology has important regional implications.

2. A distinct stratal disruption horizon is developed subparallel to bedding ~20 m above the angular unconformity along the base of the Yakataga Formation west of the Tyndall Glacier. This stratal disruption horizon could represent the base of a large, syndepositional gravity slide mass within the Yakataga Formation. However, we interpret this horizon as an out-of-sequence, younger thrust localized near the angular unconformity. We show a tentative trace for this thrust based on image interpretation, but incomplete exposure and brief field time precluded detailed mapping (Plate 2).

3. To the east of the Tyndall Glacier, the Yakataga Formation is absent and at the equivalent structural levels of the Yakataga Formation, beneath the Coal Glacier thrust, the thrust places lower Kulthieth Formation on upper Kulthieth Formation. However, on the ridge crest of the Chaix Hills, the Poul Creek Formation reappears in the footwall of the Coal Glacier thrust (Plate 2), indicating that a full section of the Kulthieth Formation and part of the lower Poul Creek is present along the Chaix Hills ridge. Nonetheless, farther east the thrust cuts downsection again and repeats the Kulthieth Formation, presumably either tipping out eastward or connecting to the next higher thrust in the stack (i.e., as shown in Plate 2).

4. Folds in the middle Kulthieth Formation are disharmonic and noncylindrical, consistent with a complex structural overprinting. Bedding and fault traces partially show this relationship in map view (Plate 2), but stereonet plots of poles to bedding show classic shotgun patterns indicative of noncylindrical folding (Fig. 8). We have not examined these folds in great detail, but the noncylindrical geometry suggests that they are the result of early northwest-plunging folds overprinted by upright approximately east-west–trending fault-related folds.

Collectively these observations suggest that the Chaix Hills thrust sheet is a composite structure with an early history of motion that produced hanging-wall exhumation and folding. This deformation was followed by syntectonic deposition of the Yakataga Formation above the angular unconformity, but younger motion subsequently deformed the Yakataga Formation to form an open syncline (Chapman et al., 2012). This younger thrust system obviously involved at least the overlying Coal Glacier thrust, but we infer that this event also produced the stratal disruption horizon along the angular unconformity as well as complex fault arrays within the Kulthieth Formation, and that these fault arrays also produced an overprinting that led to the observed noncylindrical folding within the rocks. Stereonet plots (Fig. 8) together with map relationships suggest that the noncylindrical folds are due to early northwest-plunging folds overprinted by upright approximately east-west–trending folds, the younger age of the latter inferred from the folding of the Yakataga Formation. This younger fold trend is also observed in the structurally underlying Yakataga Formation in the Yakataga anticline (Plate 2).

Coal Glacier Thrust Sheet

The Coal Glacier fault is exposed locally in the Chaix Hills and west of Tyndall Glacier, but its connections to the west and east are buried by ice cover. Where well exposed in the Icy Bay area, rocks above the Coal Glacier thrust are a relatively homoclinal, north-dipping section of the Kulthieth Formation that we tentatively correlate with the upper Kulthieth Formation. Up structural section, however, this sequence becomes complex and it is uncertain which rock units are present immediately west of Tyndall Glacier. In the eastern part of the mapped area (Plate 2), rock units are well established from direct field observations (Bruhn et al., 2004; G. Plafker, 1999, written commun. to T. Pavlis). Here moderately folded Kulthieth Formation structurally overlies the Poul Creek Formation along the ridge crest, but the Poul Creek-Kulthieth contact shows a footwall cutoff downslope, and there is complex detachment folding in the underlying upper Kulthieth Formation (Plate 2).

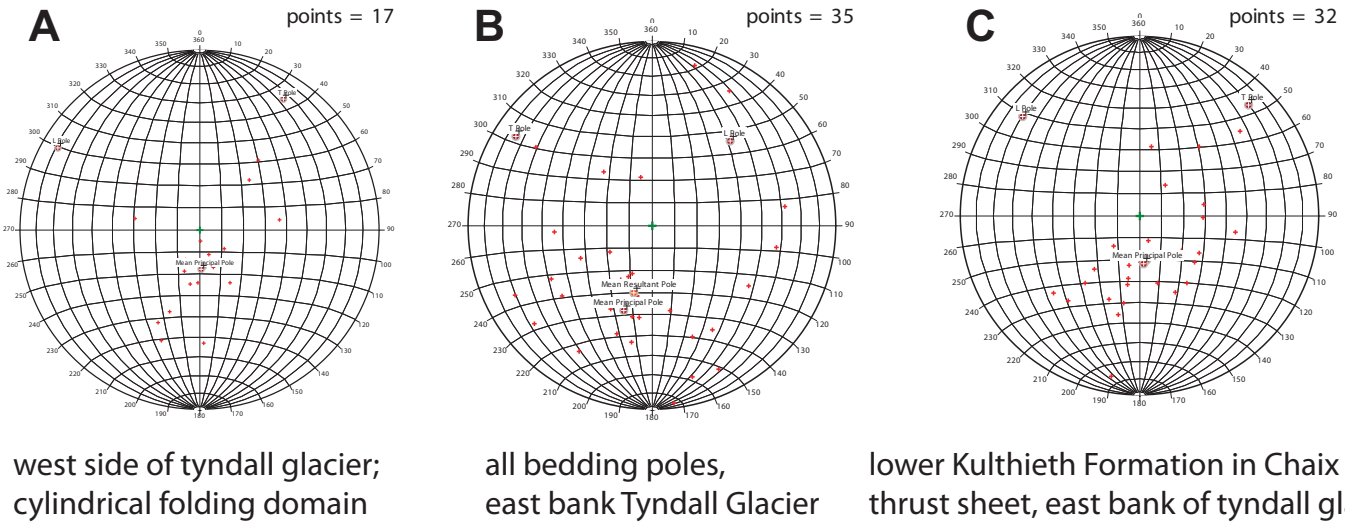

Figure 8. Equal-area, lower hemisphere stereographic projections of poles to bedding in three structural domains along the Tyndall Glacier (Plate 2). Note the cylindrical, northwest-plunging folds recognized in the Kulthieth Formation west of the Tyndall Glacier (A) and in the lower Kulthieth Formation (C) east of the Tyndall Glacier, whereas bedding in the middle and upper Kulthieth, below the angular unconformity with Yakataga Formation (B) shows a shotgun scatter pattern indicative of noncylindrical folding. See text for a discussion of the context of this observation relative to overprinting fold systems.

To the west, however, across Tyndall Glacier, we were not able to directly examine rock exposures during our field work, and rock unit identifications are based solely on reconnaissance mapping by Plafker (cited *in* Richter et al., 2006; Wilson et al., 2005; G. Plafker, 1999, written commun. to Pavlis and Bruhn), inferences from aerial photography, and views from across Tyndall valley (Plate 2). In this area, it is clear that rocks directly above the Coal Glacier fault are the Kulthieth Formation, from our own observations and appearance on satellite imagery (Plate 2). However, the Kulthieth Formation here is overlain by reddish-brown weathering, shaley rocks with conspicuous interlayered volcanic rocks, concordant intrusive rocks, or both. These reddish-brown shales display a large overturned syncline in the cliff face above Tyndall Glacier (see photo in Chapman et al., 2012; bedding traces in Plate 2). Regional maps (Richter et al., 2006) and Plafker's field map sheets (G. Plafker, 1999, written commun. to Pavlis and Bruhn) indicate that these rocks are Tertiary sedimentary rocks and associated Tertiary igneous rocks. Based on these observations and the reddish color of most of these rocks, our preferred interpretation is that these rocks are complexly deformed Poul Creek Formation with interlayered volcanic rocks, hypabyssal intrusives, or both. In addition to the basic appearance on satellite imagery, this correlation with the Poul Creek Formation is supported by two observations: (1) volcanic rocks are a common feature within Poul Creek Formation exposures ~10 km west of Tyndall Glacier (Plate 2) and these rocks appear to be similar to the igneous rocks in the cliffs above Tyndall Glacier; and (2) the exposures of the Poul Creek Formation west of Tyndall Glacier (Plate 2) are in a similar structural position relative to the Coal Glacier thrust sheet, and in our mapping we correlate these exposures as part of the same thrust sheet. This differs from the interpretation presented in Chapman et al. (2012), where the Libbey Glacier thrust is projected directly across the Tyndall Glacier.

Haydon Peak and Crater Basin Thrust Sheets

The Haydon Peak thrust and Crater Basin thrusts (Plate 2) carry three distinct assemblages in their hanging walls, all separated by faults. The Haydon Peak thrust carries a stratally disrupted metasedimentary assemblage with abundant felsic intrusives that we correlate with the Yakutat Group mélange. This interpretation is consistent with mapping by Plafker (1987; and in Richter et al., 2006) and Chapman et al. (2012). This mélange assemblage is in turn structurally overlain by a coherent, sedimentary and/or metasedimentary assemblage dominated by a rhythmically bedded sandstone-shale sequence. Bedding traces are easily mapped in this assemblage on the south face of Haydon Peak (Plate 2). From these bedding traces, it is clear from truncations that the base of the assemblage is a fault, and the geometry of some of the bed traces suggests that the rocks record at least two generations of folding. We informally use the term Haydon Peak assemblage for these rocks because of uncertainties in correlation. However, the correlation of the mélange assemblage to the Yakutat Group indicates that Yakutat terrane basement extends well west of the Samovar Hills (Chapman et al., 2012), and this correlation is used in our reconstructions for the system.

The Haydon Peak assemblage is structurally overlain by a poorly understood metamorphic assemblage referred to here as the Barkley Ridge terrane. We use terrane terminology for this assemblage because it has no clear correlative rocks and could be part of the Yakutat Group, the Chugach terrane, or the Prince William terrane. We were unable to directly observe these rocks other than from glacial float. Nonetheless, this limited analysis, together with our remote sensing and descriptions in Richter et al. (2006), suggests that this assemblage is composed of greenschist to lower amphibolite facies metasedimentary rocks and associated tonalitic intrusive rocks. We infer the Crater Basin fault between these metamorphic rocks and the Haydon Peak assemblage because of the apparent difference in metamorphic grade and structural style, but this apparent structure is not exposed in the mapped area. The Barkley Ridge terrane continues westward in exposures along the Barkley Ridge, but changes along strike. Plutonic rocks are abundant in the east (Plate 2) but largely disappear to the west. This change is accompanied by a change in structural style from rocks with a conspicuous foliation parallel to layering to a weakly foliated assemblage to the west. Near this structural transition, Richter et al. (2006) mapped a fault to distinguish these higher grade rocks from low-grade Orca Group to the west. If the Barkley Ridge terrane is part of the Yakutat terrane, this fault is the Chugach–St. Elias suture. However, if the Barkley Ridge terrane is part of the Orca Group (Prince William terrane) or Chugach terrane, the Crater Basin fault is the suture and is part of the Chugach-St. Elias fault system.

Our preferred interpretation (Plate 2) follows previous interpretations by Plafker (1987) that the Barkley Ridge terrane is a part of the Orca Group that was deeply exhumed. On satellite imagery and from aerial reconnaissance, these rocks are indistinguishable other than the apparent increase in fabric intensity from west to east, which is easily explained as the product of increasing metamorphic grade and associated ductile deformation from west to east. This interpretation is based on few data, however, and needs to be resolved by future studies.

St. Elias Thrust Sheet

The top of the structural stack is composed of crystalline rocks that underlie the Mount St. Elias massif and adjacent areas of the St. Elias–Barkley Ridge. From G. Plafker's reconnaissance mapping (written communication to Pavlis and Bruhn, 1999), analysis of satellite imagery (Chapman, 2008; Chapman et al., 2012), a mountaineering account (K. Stuwe, 1998, written commun. to Pavlis), and 1998 field observations (Pavlis, V. Sisson, and K. Stuwe), it is clear that this assemblage is composed of strongly foliated, upper amphibolite facies metabasites, unfoliated coarse-grained gabbroic rocks, and foliated granitoids, probably Eocene tonalite-granodiorite. We have observed this assemblage at three localities east of Mount St. Elias and have examined samples of these rocks from float derived from the south face of Mount St. Elias. Based on these spot observations and our reconnaissance mapping of foliation traces in the assemblage (Plate 2), it is clear that these rocks were subjected to at least two major folding events under upper amphibolite facies conditions. The metamorphic rocks are predominantly amphibolite gneiss with plagioclase-rich leucosomes interleaved with hornblende + plagioclase ± clinopyroxene melanosomes indicating upper amphibolite facies conditions during the main metamorphism (Arnold, 2010). One sample collected from this assemblage within 5 m of the Chugach–St. Elias fault, however, shows a mylonitic overprint with a distinct second generation of amphibole (Arnold, 2010). Because this texture is only seen from the sample close to the Chugach–St. Elias fault, this mylonitic overprint probably records a period of ductile deformation under upper greenschist–lower amphibolite facies conditions presumably related to Neogene movement on the Chugach–St. Elias fault.

We tentatively conclude that these high-grade mafic gneisses are parts of the Chugach or Prince William terranes that have been exhumed from greater depth by the uplift in the Mount St. Elias region. Although undated, the high-grade metamorphism is almost certainly Eocene metamorphism associated with the Chugach metamorphic complex, and thus the assemblage is part of the North American backstop. These mafic rocks may correlate with mafic schist and gneiss exposed along the southern edge of the Chugach metamorphic complex (Lull and Plafker, 1990; Bruand, 2011; Bruand et al., 2011). However, given the evidence of at least 10 km of Neogene exhumation within

this region (Enkelmann et al., 2010) and the mylonitic amphibolites near the structural contact at the base of the assemblage, the rocks may be exhumed from greater depths. Fuis et al. (1991) recognized high-velocity layers at depths of >10 km beneath the Chugach metamorphic complex near the Copper River that they interpreted as mafic underplating. However, gabbro and amphibolite are nearly indistinguishable in seismic velocity (e.g., Hacker et al., 2003), and these mafic layers could also be composites of amphibolite and gabbroic intrusive sheets. Given that thermochronology data (Spotila and Berger, 2010; Enkelmann et al., 2010) indicate at least 10 km of differential exhumation between the Copper River and the Mount Logan and Mount Elias region, we speculate that the St. Elias massif is the exhumed mafic root of the Chugach metamorphic complex; this hypothesis needs testing through further work on this metamorphic assemblage.

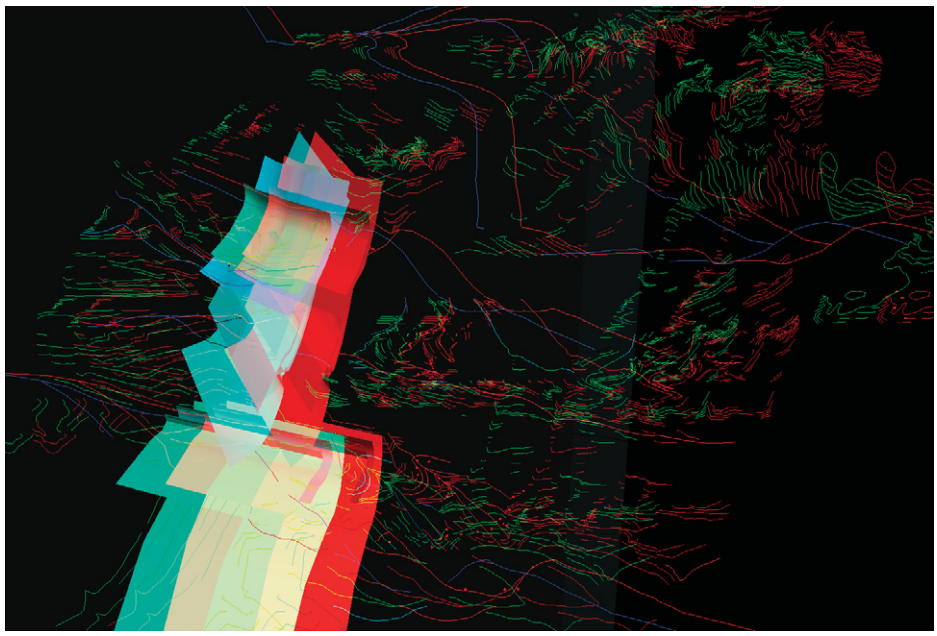

Figure 9. Three-dimensional (3D) visualization of the Icy Bay area, showing inferred fold geometries in the Icy Bay transect. The 3D surfaces are largely diagrammatic, and produced by projecting line work from cross sections and the map along fold trends. Static magenta-cyan image of these structures used the cross section in Figure 11. The figure can be viewed in 3D with cyan-magenta glasses. Compare with Supplemental File 3 (see footnote 3) to see the dramatic distinction in fold trends at different structural levels.

Synthesis of Structure in the Unmetamorphosed Fold-Thrust Belt

The Icy Bay region is a clear example of 3D structure that evolved in time (e.g., Chapman et al., 2012). Most notable is the difference in fold trends between older rocks and the Yakataga Formation; i.e., northwest-trending, but commonly noncylindrical folds in Kulthieth Formation versus west-northwest– to east-northeast–trending folds in the Yakataga Formation. This pattern is particularly striking in the Chaix Hills thrust sheet, but the regional relationship implies changes in shortening axes of as much as 60°–70° between older structures and the folds in the Yakataga Formation.

To illustrate this geometry, we produced a simplified visualization of the 3D fold geometries in the Icy Bay region (Fig. 9; Supplemental File 3[3]) emphasizing that the timing of some of these structures is not necessarily well constrained. Two prominent observations can be made from this visualization: (1) a belt of northwest-trending structures in the Kulthieth and Poul Creek Formations parallels the Crater Basin and Haydon Peak faults from the Chaix Hills, westward to the edge of the mapped area; and (2) fold axes in the syntectonic Yakataga Formation change systematically with descending structural level, i.e., west-northwest trends in the Chaix Hills thrust sheet, approximately east-west trends in the Yakataga anticline and footwall syncline of the Chaix Hills thrust, and northeast trends in the hanging wall of the Malaspina fault. This suggests a systematic change in kinematic history, evaluated further in the following.

CROSS-SECTION RESTORATION

Although all of the structures in this region show 3D complications, the western half of the Duktoth mapping transect (Plate 1) is sufficiently 2D that cross-section analysis is a useful exercise for evaluation of the finite structure. Similarly, although the Icy Bay region contains even more complex 3D structure, the structure is predominantly 2D and cross-section analysis is informative. Thus, we constructed a series of cross sections through this region, and analyzed their validity through restorations. Figures 10 and 11 show our synthesis of this analysis as two summary cross sections.

The onshore subsurface structure for both sections (Figs. 10 and 11) is speculative because there is no subsurface structural control other than a projection of the top of basement landward from offshore seismic data (Worthington et al., 2010), seven onshore oil exploration wells, earthquake locations, and passive seismic imaging. To constrain the interpretation, we made two simplifying assumptions.

1. We assume that significant duplexing occurred in the subsurface to account for the relatively large structural thickness in the sections (~15–18 km across the sections) relative to the thickness of the preorogenic strata (4–5 km) and the length of the deformed sections (<70 km). That is, given the structural thickness, the stratigraphic thicknesses, and the dip of major structures at the surface, there is excess cross-sectional area at depth. Wallace (2008) used a duplex assumption in his reconstructions, but thought that basement was involved in the duplex. Here we assume that, other than the upper thrust sheets in the Icy Bay area, the duplexing is limited to the sedimentary cover because there is no evidence for shallow basement in STEEP seismic data (e.g., Worthington et al., 2010, 2012). In addition, there is no

[3]Supplemental File 3. Move (.mve) file that can be viewed using the free windows or Linux viewer available for download at http://www.mve.com/resources/downloads. Note that the .mve file shows a full three-dimensional (3D) representation of the line work in Plate 2 as well as more regional structures together with the deformed sections in Figure 11 and Plate 2 in their true 3D positions. This file contains different surface representations than Figure 9 through use of projected line work from the more detailed cross section in Plate 2, but both Figure 9 and this visualization illustrate the dramatic distinction in fold trends at different structural levels. Projected surfaces are labeled, but the color scheme is yellow—bedding surfaces in Yakataga Formation, dark blue—basal Yakataga angular unconformity, green—bedding surfaces in Kulthieth Formation, pale blue—Poul Creek–Kulthieth contact, and red—Malaspina fault. If you are viewing the PDF of this paper or reading it offline, please visit http://dx.doi.org/10.1130/GES00753.S3 or the full-text article on www.gsapubs.org to view Supplemental File 3.

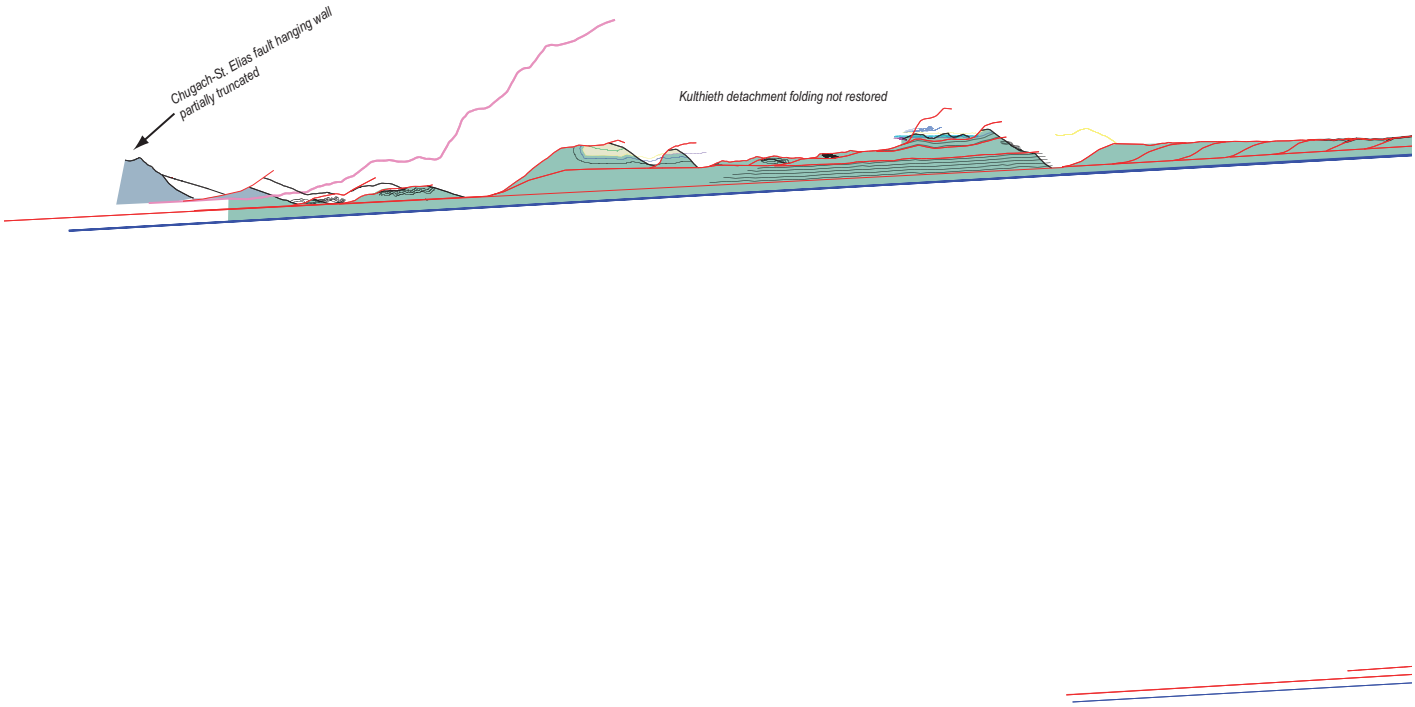

Figure 10 (*continued on following page*). Regional cross section and restoration of A–A′ from Plate 1 (s.l. is sea level). The deformed section is constructed from onshore geology and projection of STEEP (St. Elias Erosion and Tectonics Project) seismic line 17 onto the profile. Subsurface geometry is relatively speculative, but the section is restored in two phases: removing 29 km of shortening in the outer thrust systems transferred to an inferred duplex in the Kulthieth Formation (middle section) and a total restoration of the section (upper figure) excluding complex folds of the Kosakuts thrust system.

evidence for shallow high-velocity material suggestive of basement onshore in passive seismic imaging (G. Pavlis, 2011, personal commun.). Development of a duplex is also consistent with our field observations in the Duktoth transect where the Kosakuts thrust system shows extensive duplex development.

2. For the Icy Bay transect, all of the structures are on land and do not require significant assumptions tying onshore and offshore structure. For the Duktoth transect, however, the onshore and offshore structures are intimately linked and our section extends onshore geology to offshore using seismic images from the Worthington et al. (2010) STEEP line 16 (Fig. 10). In the absence of the offshore seismic data, a simple stacked, imbricate thrust model could have been used to match the onshore geology. However, we rejected this interpretation for the Duktoth section because Worthington et al. (2010) showed that the offshore fold-thrust system accounts for <10–12 km of shortening. This indicates that a simple imbricate thrust-stacking scenario with a major thrust at the deformation front taking up most of the recent deformation is not allowable. Thus, because we know hundreds of kilometers of convergence have been absorbed in the orogen during the Neogene (Plafker, 1987), we assume that most of that convergence is taken up on onshore structures, or structures along the present coastline.

Duktoth River Transect

Figure 10 shows one regional reconstruction of several structural restorations that were considered. The deformed section (Fig. 10) shows both an outer and inner duplex; the outer duplex results from an assumption that a large fraction of the section is underthrust to form the duplex, whereas the inner duplex assumes structures

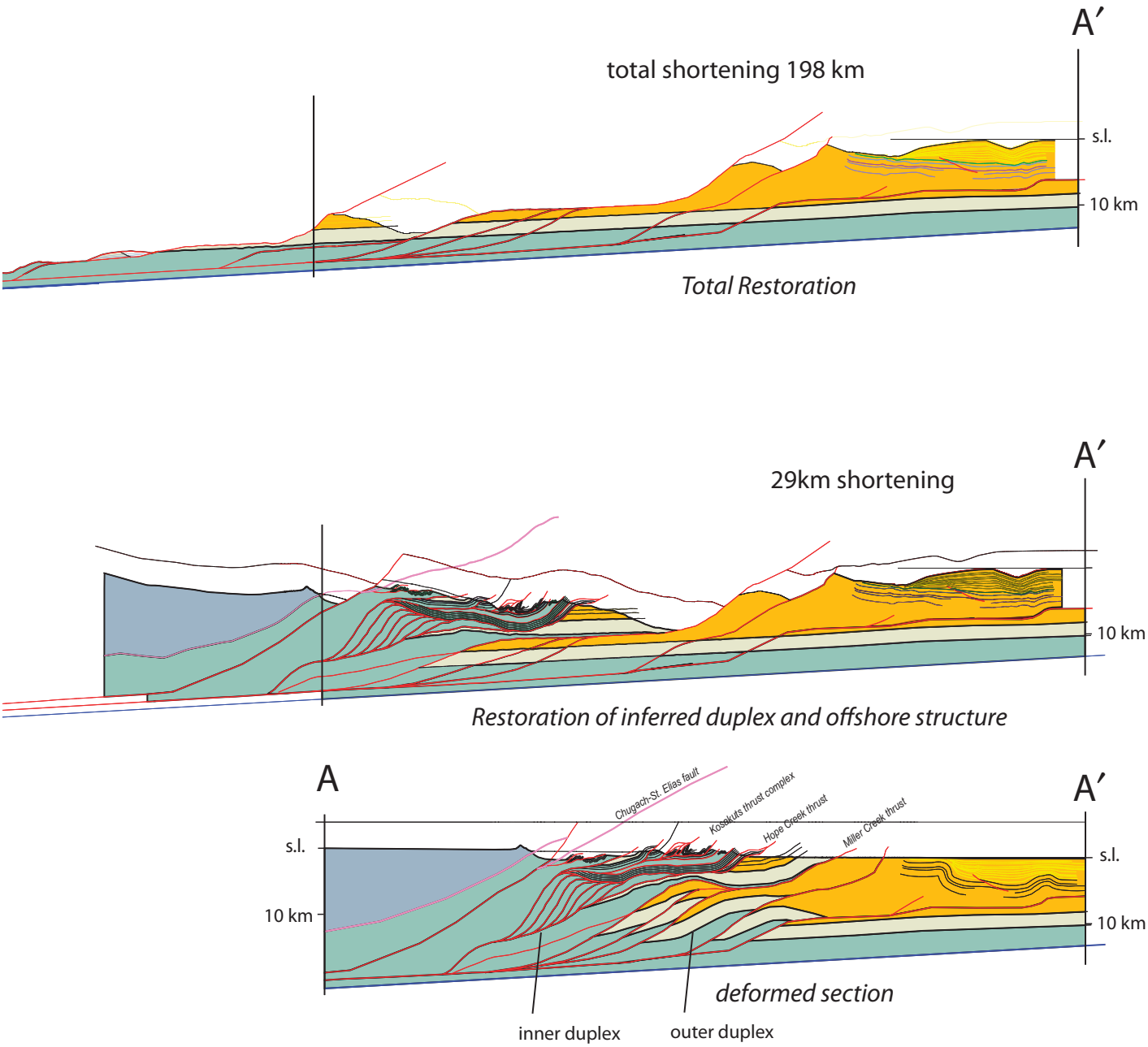

similar to the observed duplex along the Kosakuts thrust that involve only the Kulthieth formation. The restoration process involved hundreds of steps, but we show two phases of the restoration for clarity (Fig. 10).

Phase 1 of the restoration is the best constrained part of the restoration, with two components: (1) an outer section that is well defined by seismic line STEEP 16, which shows particularly well-imaged growth strata (see Worthington et al., 2010); and (2) the inboard part of the section that restores deformation (translation and folding) along an inferred thrust located along the shoreline, together with part of the cumulative motion on the Miller Creek fault that is transferred to a subsurface duplex beneath the mountains. In addition, we infer an out-of-sequence thrust along the Bering Glacier (following Bruhn et al., 2004, 2010).

In the outer part of the section, we restore two offshore folds: a younger, nearshore fold that is modeled as a trishear fold, and an older fold, buried beneath younger strata, that is restored as a fault bend fold with the assumption that this structure transfers slip to structures at the deformation front (e.g., structures on seismic line STEEP 1 described by Worthington et al., 2010). The total shortening of 8 km in this offshore section is similar to that determined by Worthington et al. (2010) for seismic line STEEP 1, which is just to the east and partially overlaps the structures imaged in line STEEP 16 (Supplemental File 2 [see footnote 2]).

The onshore part of this phase of the restoration assumes slip on an inferred buried thrust near the coastline and slip along the Miller Creek fault, which extends downdip into a duplex involving the preorogenic section along with part of the synorogenic Yakataga Formation. This duplex is undoubtedly an oversimplification of the subsurface structure, but restoration of these structures accounts for 29 km of

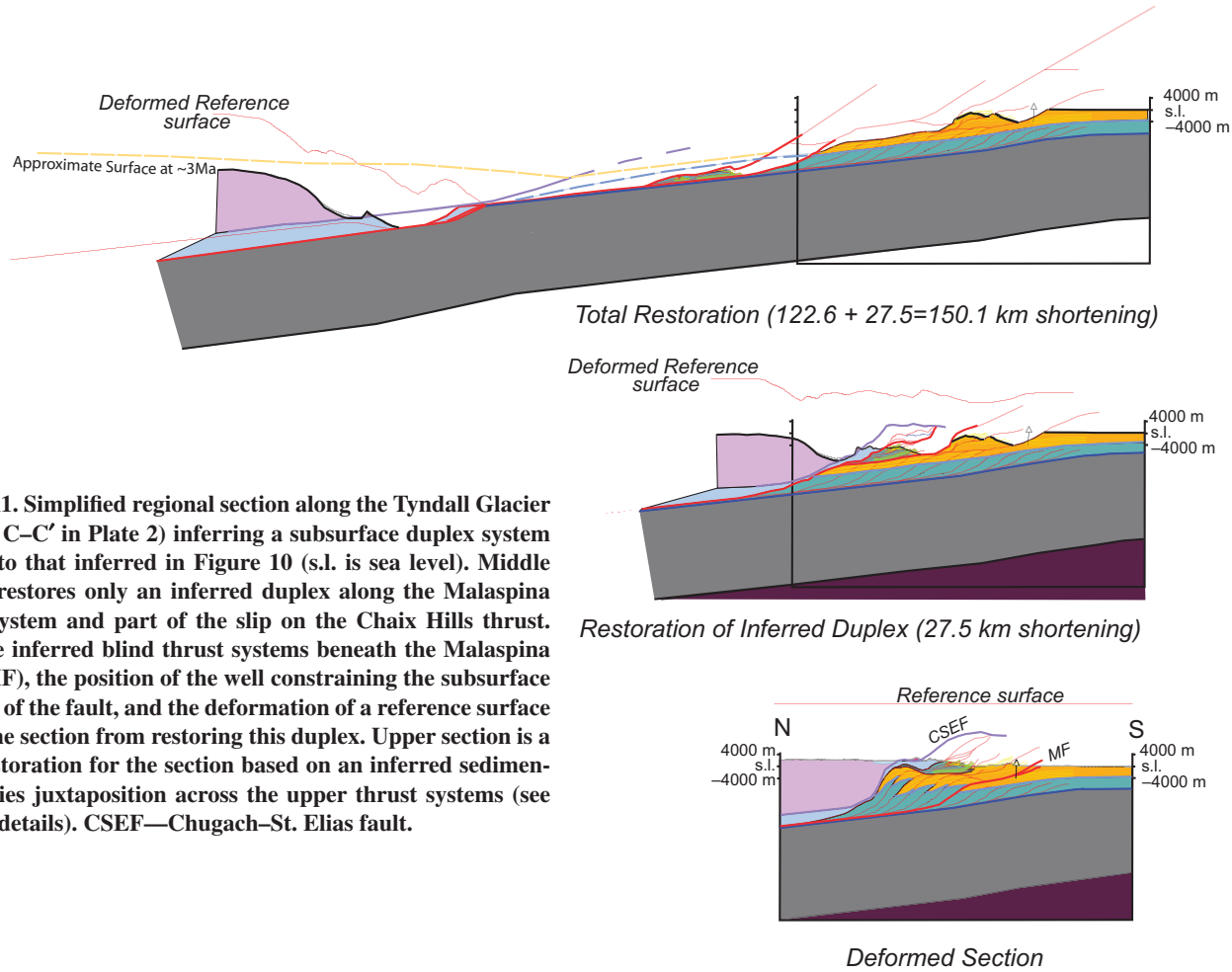

Figure 11. Simplified regional section along the Tyndall Glacier (section C–C′ in Plate 2) inferring a subsurface duplex system similar to that inferred in Figure 10 (s.l. is sea level). Middle section restores only an inferred duplex along the Malaspina thrust system and part of the slip on the Chaix Hills thrust. Note the inferred blind thrust systems beneath the Malaspina fault (MF), the position of the well constraining the subsurface position of the fault, and the deformation of a reference surface above the section from restoring this duplex. Upper section is a total restoration for the section based on an inferred sedimentary facies juxtaposition across the upper thrust systems (see text for details). CSEF—Chugach–St. Elias fault.

shortening, with only a partial restoration of slip on the Miller Creek fault at this phase.

Phase 2 of the restoration restores all of the major structures along the section, including the Hope Creek fault, the Kosakuts fault system, and the unnamed thrust beneath the Bering Glacier. Like the outer part of the section modeled in phase 1, we assume a significant duplex beneath the Hope Creek thrust sheet, but we assume that this duplex is developed in the Kulthieth Formation. This assumption seems reasonable, given surface geologic observations of the Kosakuts thrust system. We have not attempted to restore the entire fold system within the Kosakuts thrust complex because these folds are too complex to restore with any certainty.

Key features of this restoration include: (1) a total shortening across the section of ~200 km; (2) an inferred ramp-flat section of the Hope Creek thrust sheet that is strongly suggested by the hanging-wall flat above the Hope Creek fault, the Poul Creek slice located along the fault, and the subsurface geometry required to accommodate these features; and (3) an inferred duplex beneath the Hope Creek thrust that accounts for almost 40 km of the total shortening and restoration of displacement along the Hope Creek fault. The shortening estimate in this section is a minimum because additional shortening may have been accommodated on the Hope Creek fault and the unnamed upper thrust. Moreover, if the inferred duplex horses were limited to a thinner part of the section (e.g., middle Kulthieth only), the section could be restored to show greater shortening.

Icy Bay Transect

The Icy Bay transect shows significant along-strike changes in structure; there are out-of-sequence structures with fold trends that do not match the mapped thrusts, and there are uncertainties in correlation of rock units at the top of the structural stack. These 3D complications have important implications (see following), but like the Duktoth section, it is informative to analyze the system in cross sections approximately parallel to the present convergence direction.

Figure 11 shows a cross section constructed along the Tyndall Glacier–Taan Fiord transect perpendicular to the strike of the Malaspina fault. The only subsurface constraints are our analysis of the Chaix Hills #1 well and our assumption that the active thrust décollement projects downward through the aftershock zone to the primary rupture zone of the 1979 earthquake. Our depth estimate for the main thrust is shallower than that of Estabrook et al. (1992) because we have used a revised velocity model and associated earthquake relocations based on the STEEP seismic array (G. Pavlis, 2010, personal commun.).

Like the Duktoth area, we explored numerous options for the inferred subsurface structure, and Figure 11 shows one of the simplest of these options; for example, the section does not deal with the possibility that the Coal Glacier thrust is a younger, out-of-sequence thrust. As for the Duktoth section (Fig. 10), we infer a duplex beneath the main fold-thrust system, and show two phases to the restoration: (1) an initial phase that restores the inferred duplex; and (2) a total restoration that restores all of the known thrust systems exposed at the surface.

The initial phase of the restoration accounts for only 27.5 km of shortening accommodated

exclusively on the Malaspina fault and an imbricate on the Malaspina fault, transferred downdip to a simple duplex. Two observations are important from this phase of the restoration. First, the shortening on the Malaspina fault system could easily have occurred in <1 m.y. if the thrust belt accommodates a significant fraction of the known Yakutat–southern Alaskan convergence rate (~47 mm/yr) (e.g., Elliott et al., 2010). Second, the restoration of the inferred duplex predicts a large component of uplift across the fold-thrust belt during the same interval; for example, note the deflection of the reference surface in the restoration indicating a broad area of ~3 km of uplift, and localized uplift near Mount St. Elias of ~5 km, areas of known rapid exhumation based on thermochronology (e.g., Berger et al., 2008a, 2008b; Enkelmann et al., 2009, 2010; Spotila and Berger, 2010).

In the second phase of the restoration, we show a potential scenario that represents the minimum slip required to restore the basement-involved thrust sheets at the top of the structural stack. In this restoration, we assume that the original sedimentary cover had a taper in thickness comparable to the undeformed rocks that cross the Dangerous River zone offshore of Yakutat (e.g., see Risley, 1992; Worthington et al., 2012), or ~100 km. Using this assumption, the minimum convergence within the Icy Bay section is ~150 km. Note that if we project a surface from just above the trailing edge of the section, assuming a simple tapered wedge (yellow line, upper section, Fig. 11), the rocks now exposed at the surface near Mount St. Elias would have been at depths as much as 10 km as recently as 3 Ma at full convergence rates. Thus, although this section is highly simplified, it may explain the occurrence of the mylonitic amphibolites along the Chugach–St. Elias fault as well as the young detrital zircon fission track ages from this area (Enkelmann et al., 2010).

DISCUSSION

Comparison to Previous Shortening Estimates for the Orogen with Implications for Larger Scale Tectonic Processes

Comparing the cross sections produced during this project with those of Meigs et al. (2008) and Wallace (2008) illustrates the impact of assumptions concerning rock units and structural style when balancing cross sections. Both previous studies estimated a relatively small amount of shortening for the fold-thrust belt: 36 km for Wallace's (2008) section and 82 km for that of Meigs et al. (2008). These shortening estimates are far less than our estimate of ~200 km for the Duktoth section (Fig. 10), primarily because of different assumptions concerning the subsurface geology. Wallace (2008) assumed a duplex fault system similar to that in our sections, but he assumed that the duplex involved crystalline basement, which filled much of the space in the subsurface. As a result, he estimated a much lower total shortening. Meigs et al. (2008) assumed a simple ramp-flat, stacked thrust system, with the only complication from an out-of-sequence thrust, the Miller Creek thrust; their section also assumed a relatively shallow basement and associated décollement, which allowed the construction of a relatively simple cross section, albeit with a relatively low shortening as a result.

The effect of subsurface assumptions can be illustrated by simple cross-sectional area calculations. In Figure 10, the cross-sectional area of deformed, preorogenic strata is ~1000 km^2. Given the ~5 km thickness of preorogenic strata, this equates to ~200 km of shortening, assuming a simple restoration to predeformational area. This estimate is indistinguishable from the estimate derived from Figure 10. This is not surprising, however, given the subsurface assumptions of duplexing in the Kulthieth Formation that restores most of the shortening as slices of the preorogenic section; i.e., excess cross-sectional area at depth is balanced by underplating of the preorogenic strata in the section. This result illustrates an important feature of the restoration in Figure 10. Had we assumed that all excess cross-sectional area was due to duplexing in a limited part of the section, such as ~1 km of middle Kulthieth strata, the total shortening could approach 1000 km (restoration of 1-km-thick horses across 1000 km to produce 1000 km^2). In contrast, had we assumed that all duplexes involved the entire ~10 km section, the total shortening could be as low as 100 km. We consider these theoretical values end members, because we observe duplexes within the middle Kulthieth Formation, but also recognize imbrications of the entire stratigraphic section across the thrust belt. These order of magnitude calculations illustrate the range of solutions possible in the absence of subsurface data and demonstrate that it is difficult to account for significantly more than ~200 km of shortening in Figure 10 unless virtually all of the excess cross-sectional area was composed of only a fraction of the total stratigraphic section.

This simple analysis is significant because all of these shortening estimates are low relative to the known amount of convergence in the orogen. There is extensive evidence that the Yakutat terrane and Pacific plate have both moved northward at least 1000 km during the past ~20 m.y. (e.g., Plafker et al., 1994). Part of that motion was taken up by subduction of oceanic crust before the thicker and more buoyant Yakutat terrane arrived at the trench. However, today the buoyant lithosphere of the Yakutat terrane extends at least 600 km beneath southern Alaska (Ferris et al., 2003; Eberhart-Phillips et al., 2006). Thus, most of the ~600 km of underthrusting indicated by the subducted Yakutat terrane must have been taken up in the St. Elias fold-thrust belt because the area above the subducting Yakutat terrane shows little Neogene deformation (e.g., Plafker et al., 1994), suggesting microplate behavior with the plate boundary in the St. Elias orogen. Moreover, because the Yakutat terrane was proximal to North America from the Eocene, there was a significant sedimentary source for the terrane throughout its Neogene history (e.g., Plafker, 1987). Thus, the subducted Yakutat lithosphere should have been blanketed by a thick preorogenic cover sequence and this cover should have been incorporated in the thrust belt, yet our reconstructions do not account for these missing strata.

These relationships lead to a question: where are the sedimentary rocks that should have been offscraped into the thrust belt during this convergence? There are several possibilities: (1) we underestimate the shortening because of unconstrained convergence along bed-parallel faults; (2) sedimentary cover was very thin at the leading edge of the Yakutat terrane, and the area balance issues are overestimated; (3) sediment accreted early in the convergence history was uplifted, eroded, and recycled during convergence, destroying all evidence that could be recognized in a restored section; (4) sediment was extruded parallel to the margin during convergence, and now forms part of the Alaskan-Aleutian forearc; and (5) large amounts of sediment have been subducted beneath the margin.

Of these possibilities, we suggest that subduction of sedimentary material may be one of the most significant factors contributing to this area mismatch. Fruehn et al. (1999) documented extensive tectonic erosion within the eastern Alaska–Aleutian forearc that they related to the collision of the Yakutat terrane. Part of this subducted forearc material as well as Neogene sedimentary cover on the Pacific plate may have been underplated beneath the forearc high (e.g., Pavlis and Bruhn, 1983; Ye et al., 1997), but based on the data of Fruehn et al. (1999), it is difficult to find an area within the eastern Alaska–Aleutian forearc where missing rocks from the Yakutat collision could be incorporated as a laterally extruded wedge. An independent data set reported by Rossi et al. (2006) and Eberhart-Philips et al. (2006) may provide the answer with evidence for unusual physical properties in the mantle wedge beneath the eastern Alaska–Aleutian arc. Specifically, Rossi

et al. (2006) reported unusually low Vp/Vs (compressional to shear wave velocity) ratios in the mantle wedge at the leading edge of the subducting Yakutat terrane. The reported Vp/Vs values are not consistent with normal upper mantle values and are most easily explained by large volumes of rock with free quartz (Rossi et al., 2006). We suggest that this observation is consistent with extensive sediment subduction along the margin that could include both subduction of forearc material (as suggested by Fruehn et al., 1999) and sedimentary cover carried on Yakutat terrane to account for part of the mismatch in accreted preorogenic strata versus likely preorogenic volumes.

This conclusion is speculative from available data, but we suggest that future studies should more fully analyze this mass balance. The eastern Alaska–Aleutian arc is an unusual, nearly closed system in which synorogenic products are near their source and the scale of the collided block is such that we can make estimates of preorogenic versus synorogenic volumes to potentially produce a mass balance. This type of analysis might ultimately be key to understanding amounts of sediment subduction versus accretion in these settings and their effects on upper mantle processes.

Implications of Cross-Section Restoration to Exhumation Patterns

Berger et al. (2008b) and Berger and Spotila (2008) used low-temperature thermochronology data to infer two important features of the St. Elias fold-thrust belt. (1) They noted an age discordance across the Bagley Icefield and therefore inferred that a young backthrust had developed along the icefield trough (Fig. 2) and that this backthrust was potentially activated as a direct result of glacial exhumation. (2) They noted that the youngest cooling ages were correlated to the area between the modern glacial equilibrium line altitude (ELA) and an inferred Pleistocene ELA, and used this correlation to infer a cause-effect relationship, whereby erosion concentrated at the ELA led to the maximum exhumation at this position. Enkelmann et al. (2010) proposed alternative interpretations, suggesting that rapid exhumation occurred in the footwall of the proposed backthrust and that some of the young cooling ages in the south are only partially reset. The cross-section restorations reported here allow reexamination of these issues from our structural analyses.

Exhumation Focused at the Average ELA?

The Berger and Spotila (2008) hypothesis for focused exhumation localized at the ELA is consistent with models for glacial erosion because basal sliding rates are a maximum at the ELA and erosion rate typically scales to basal sliding velocity (Hallet, 1979; Hallet et al., 1996; MacGregor et al., 2000; Alley et al., 2003). The process can only be effective, however, if there are structural feedbacks to produce uplift in association with erosion, because glaciers, like rivers, are limited in their ability to erode in the absence of uplift. That is, although glaciers may be more efficient as erosional agents, they can only excavate a modest depression in the absence of uplift (Alley et al., 2003). Thus, like rivers, glacial exhumation rates are primarily controlled by tectonic rates unless tectonic rates exceed erosion rates.

Our cross sections suggest that duplex faulting stacked tabular bodies of rock at depth, focusing uplift and hence erosion within the core rather than at the leading edge of the foreland fold-thrust belt. We infer that this process is the underlying mechanism for vertical upwelling of rocks and the presence of young exhumation ages within the interior of the orogen (e.g., Berger and Spotila, 2008). Glacial erosion may have partly triggered the mechanical instability that localized duplexing at depth by decreasing the load of the overburden that resulted in duplexing of thrust sheets that created uplift from below. However, glacial erosion may be only part of the process responsible for young uplift (Pliocene and younger) in the interior of the orogen (e.g., Enkelmann et al., 2010). Several studies, including ours, have noted the importance of northeast-trending thrust faults that are the youngest structures in the foreland belt. These faults include, from west to east, the thrust fault boundary beneath the Bering Glacier (Bruhn et al., 2004, 2010; Chapman et al., 2011), faults in the offshore Pamplona belt (Worthington et al., 2010) that extend beneath the tectonic highland of the Guyot and Yahtse Glaciers just west of Icy Bay (Bruhn et al., 2009), and the Malaspina and adjacent imbricate faults that are concealed beneath the Malaspina Glacier (Plafker, 1987; Bruhn et al., 2004; Chapman et al., 2008; Elliott, 2011; Cotton et al., 2011). These faults profoundly affect duplexing at depth within the fold-thrust belt and presumably formed when the leading edge of the subduction décollement migrated eastward to establish a more stable geometry with respect to the transition from transform to convergent motion along the plate boundary. This scenario is broadly consistent with that proposed for the pattern of exhumation by Berger and Spotila (2008), but is also consistent with the interpretation by Enkelmann et al. (2010), who proposed that the exhumation pattern in the interior of the fold-thrust belt is controlled more by tectonic overprinting rather than glacial processes.

Backthrust Hypothesis

The Berger et al. (2008a) backthrust model was used in Chapman et al. (2008) to infer that the Bagley-Bering glacier system may play a role similar to that of rivers in Central Asia (e.g., Pavlis et al., 1997), where the backthrust delivers mass to the ice stream and the hanging wall is carried away as rapidly as mass is delivered to the mountain front along the backthrust. If true, this mechanism has important implications for the coupling of tectonic and erosional processes, particularly if this backthrust was activated as a result of glacial exhumation (e.g., Berger et al., 2008b; Chapman et al., 2008). Nonetheless, the results of this study raise some doubt about this conclusion. In particular, the cross-section restorations presented here indicate that although the inferred backthrust is allowable, it is not required by available data.

To illustrate this issue, we show two simplified cross-section reconstruction scenarios for recent convergence in the Duktoth section in Figure 12: a simple duplex (model A) and a paired forethrust and backthrust system (model B). We added a horizontal loose line (pink line, model A; blue line model B; Fig. 12) to each cross section and then partially restored each section to remove ~17 km of shortening. In both models we first restored 7 km of slip on offshore structures, and 10 km of slip on either a backthrust (model B) or the forethrust (model A). In model A we included two subsurface horses on a pair of foreland-vergent thrusts to form a duplex, whereas in model B we used simple slip restorations to the forethrust and backthrust. For simplicity, we did not restore slip on any of the smaller structures within the upper fold-thrust belt above the main décollement level. We graphed the difference between the original loose line and the deformed loose line to provide an estimate of uplift along the length of the cross section (magenta line model A; blue line model B). In the upper panel of Figure 12, we compare these uplift estimates for the two models with exhumation estimates since 1 Ma and 0.5 Ma using the exhumation rates estimated by Berger et al. (2008a, 2008b) and Spotila and Berger (2010). Although we cannot determine the exact amount of time needed for ~17 km of slip, we suggest that 0.5–1 m.y. is a reasonably conservative estimate based on geodectic rates of shortening (Elliott et al., 2010).

Regardless of the exact numbers, the restorations provide enough data for a first-order comparison to the thermochronology data, recognizing that uplift is overestimated in the models because they do not include isostatic adjustments. As noted herein, a simple duplex (model A, Figs. 12 and 10) can explain the

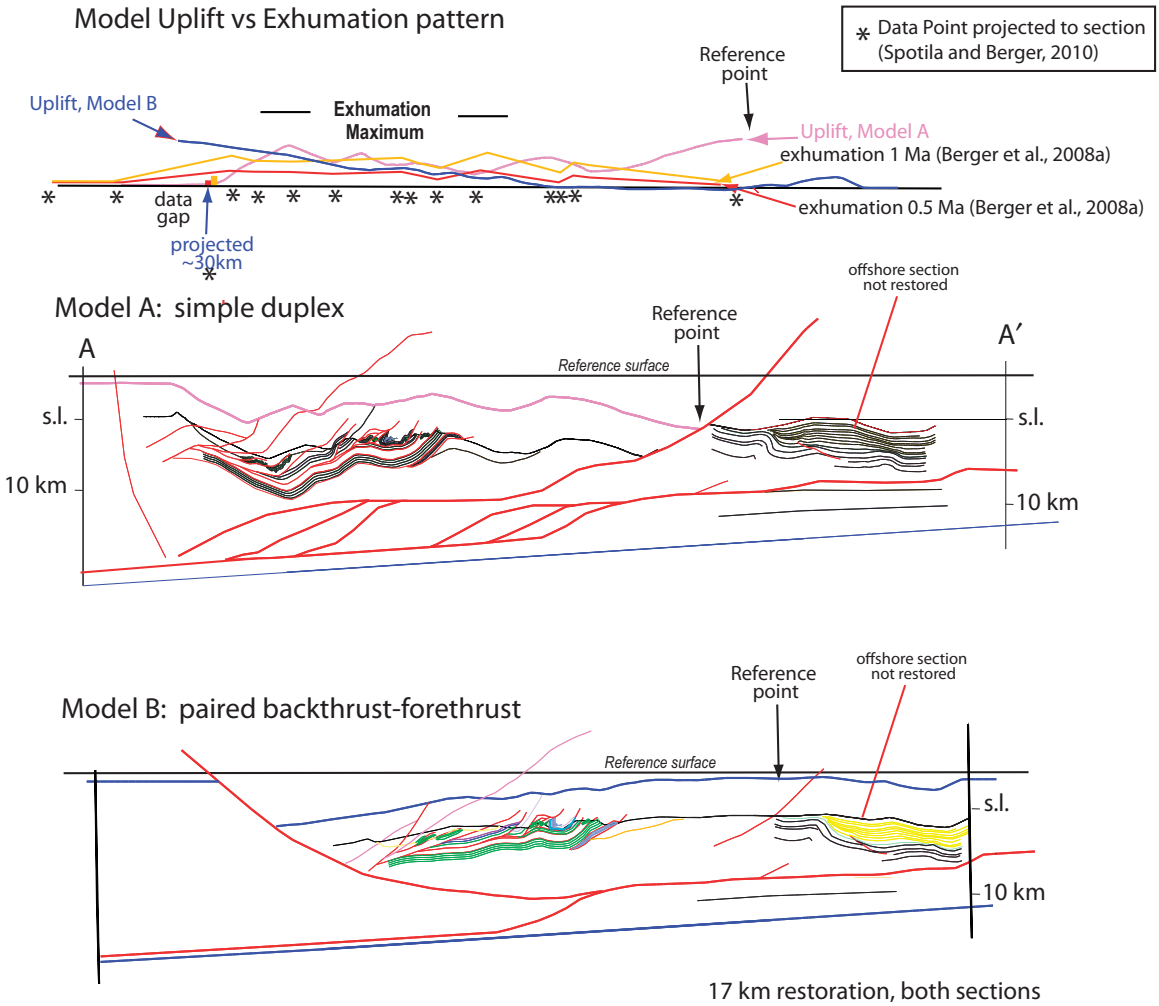

Figure 12. Simplified versions of the cross section in Figure 10 (bottom) illustrating the distinction in uplift pattern produced by a simple duplex (model A) versus a paired forethrust-backthrust system (model B) in comparison to Pleistocene exhumation rates estimated from apatite U-Th-He dating (Berger et al., 2008a; Spotila and Berger, 2010) (s.l. is sea level). Exhumation patterns are shown as a generalized curve constrained by the Spotila and Berger (2010) exhumation rate estimates projected onto the section line (data points at asterisks). Both models A and B show restoration of 17 km of shortening with 7 km of shortening on offshore faults (consistent with Fig. 10) and the remaining 10 km of slip transferred to a frontal thrust (model A) or a backthrust (model B). At modern geodetic rates, this shortening is ~0.4–0.5 m.y. of deformation. Both restorations show deflection of a loose line reference surface above the cross section, and the deflection of this surface is shown as uplift in the upper figure (magenta line, model A; blue line, model B). The inferred uplift is undoubtedly an overestimate because isostasy is not included, but is comparable to 0.5 and 1.0 m.y. of exhumation (red and orange lines, respectively) estimated by thermochronology with caveats for each model (see text).

observed exhumation pattern as a consequence of an antiformal uplift that is broadly consistent with the observed exhumation pattern (red and orange lines, top panel, Fig. 12). Nonetheless, in this scenario there is an apparent discrepancy between inferred uplift versus exhumation at the southern end (right side, Fig. 12) of the profile. That is, model A predicts significant uplift in the hanging wall of the main north-dipping, active thrust along the southern edge of the system, yet observed exhumation rates in this area are low, in apparent conflict with model A. However, this apparent conflict does not invalidate this model because any foreland-vergent thrust system will display this pattern and two factors can mask this uplift in an exhumation signal: (1) thrust loading and offshore sedimentation produce an isostatic depression at the thrust front, which would negate a large part of the uplift signal; (2) in this area only the Yakataga Formation is involved in the deformation (Fig. 10) and the oldest exposed rocks are the Poul Creek Formation along strike to the east, indicating that recent exhumation has been entirely from erosion of the synorogenic Yakataga Formation (Fig. 2; Plate 1). Together these factors could mask an exhumation signal because the thrust is exhuming synorogenic sediments that may not have been buried deeply enough to reset the thermochronometers.

The forethrust and backthrust model (blue line, top Fig. 12) also matches parts of the exhumation pattern well, but has significant discrepancy to the north (left) side of the profile (Fig. 12). Specifically, the maximum uplift in this model increases toward the backthrust and predicts 2–3 times more uplift than the exhumation estimated at this site (left side blue line, top Fig. 12). Admittedly, the key area to test this model

is essentially a gap (upper left, Fig. 12) in the Spotila and Berger (2010) data with only two samples close enough to the Bagley Icefield valley to catch the edge of the inferred uplift. These samples yielded older ages (1.28 and 1.96 Ma) relative to nearby samples closer to the Chugach–St. Elias fault (0.81 and 0.58 Ma), but the spatial discordance is deceptive because there are also elevation differences among these samples (Spotila and Berger, 2010). Nonetheless, projecting these data ~30 km along strike suggests that the data deviate from model B (exhumation shown as bars above blue arrow, top Fig. 12). More important, however, is that when the uplift rate is greater than the exhumation rate there is a net elevation increase in any orogen, and some of the highest peaks in the orogen occur along the Barkley Ridge, the area where model B predicts maximum uplift. Thus, the modern topography is consistent with model B. Nonetheless, there are extensive detrital zircon fission track data from glaciers that sample this area (Enkelmann et al., 2008, 2010), and those data indicate deep Pliocene–Pleistocene exhumation only in the Mount St. Elias–Mount Logan region (Fig. 2). Comparing the zircon fission track data to the apatite He data used for exhumation estimates in Figure 12 is difficult because of the large difference in closure temperature. However, at the least this scenario indicates that if there is a backthrust along the Bagley Icefield, its net slip must be a small fraction of the Pliocene–Pleistocene convergence or zircon fission tracks would record young ages all along the backthrust. This interpretation is allowable if the backthrust is very young (<<1 m.y.), which was favored by Berger et al. (2008b). Alternatively, the backthrust system is more long lived, but its net slip increases from west to east or contains localized complications from transpression in the Mount St. Elias–Mount Logan region, an interpretation that was favored by Spotila and Berger (2010).

Collectively, these observations suggest that the duplex model provides the simplest explanation for the exhumation pattern recognized by Berger and Spotila (2008) and Spotila and Berger (2010), with the exception of the Mount Logan–Mount St. Elias region, where the work of Enkelmann et al. (2010) and our observations of metamorphic assemblages imply greater exhumation consistent with a backthrust or transpressional effects. This conclusion is tentative, however, because more thermochronology data are needed along the Bagley Icefield trough, where the backthrust model predicts greater exhumation than the duplex model.

In one sense, the distinction between a backthrust and the back limb of an antiformal stack is subtle in terms of tectonic processes that interact with surface processes. In either case, rock uplift is produced to the south of what is now the Bagley Icefield trough, and erosion can deliver mass to the Bagley ice stream as well as to the south. It is conceivable that both processes are active, i.e., a backthrust operating in conjunction with the development of the antiformal stack. Ultimately the distinction is important for understanding the overall mechanics of the fold-thrust system as it has evolved under high exhumation rates, and future studies should consider this problem.

3D Deformational History

Although 2D cross-sectional restoration of the fold-thrust belt provides insight on the interplay of uplift and exhumation, the deformation in the orogen is distinctly 3D with both lateral transport and oblique-contraction. The 3D processes introduce complexities that are not trivial, but play an important role in the tectonics of the system. The evidence for 3D structure is different within our two transects and this distinction is important in restoration of the history.

3D Processes in Duktoth Transect

In the Duktoth transect, the principal 3D structural element is the development of northwest-plunging synclines in the hanging walls of the Miller Creek and Hope Creek thrusts (Plate 1; Fig. 7; Supplemental File 2 [see footnote 2]). These folds could indicate lateral ramps in the thrust system at depth or blind structures to the east in the unmapped areas largely covered in ice (Fig. 2). However, there is evidence suggesting that the northwest-trending folds are related to relatively young, out-of-sequence, northeast-striking thrust systems that transfer slip to depth, probably associated with a growing antiformal stack. (1) In Chapman et al. (2008), evidence was presented that there is Quaternary, northwest-directed tilting along the Duktoth River valley and that there may be active faulting along the Hope Creek fault associated with this tilting. This is consistent with a conclusion that the northwest-trending folds are actively growing, and would indicate active northwest tilting in the hanging wall of a northwest-dipping thrust system. (2) GPS studies indicate that an active thrust system is within this general region, and would account for observed velocity gradients (Elliott, 2011). (3) Orientation data from the folds in the Kosakuts thrust complex show a general approximately east-west trend for fold systems developed during motion on that thrust system, yet these fold trends are ~45° from the northwest trend of the two large-scale synclines. This suggests strongly that the northwest-trending folds are younger and superimposed on older, approximately east-west–trending structures. (4) The northwest-trending syncline above the Miller Creek thrust as well as northeast-trending folds in the footwall of the Miller Creek fault are all developed in the Yakataga Formation, indicating a relatively young age for these structures.

One implication of this interpretation of the younger, onshore structure in the Duktoth River area is a potential link to offshore structure and the 3D structure that produced the regional structural high that Wallace (2008) referred to as the Dahlgren anticlinorium. The Dahlgren anticlinorium is a structural high centered on a modern topographic high between the deep glacial valley of Icy Bay and the relatively subdued terrain between the Bering Glacier and the Duktoth River. This topographic high is largely buried beneath ice, but the area contains the highest peaks outboard of the suture, Yaga Peak (~2700 m) and Mount Leeper (~3000 m). We suggest that this topographic high is not coincidental, rather the topographic high developed because northeast-trending, out-of-sequence structures (Hope Creek, Boulder Creek, and Yaga Peak) as well as other structures have built this structural high in relatively recent times. As modeled in our cross section to the west (Fig. 10), this structural high is probably a manifestation of underplating (duplex formation) at depth with structures reaching the surface to the south and along the coast. Thus, we infer that the northwest-plunging synclines along the Duktoth River are, in part, manifestations of development of this anticlinorium.

Further evidence for out-of-sequence, northeast-trending structures building the Dahlgren anticlinorium was presented by Bruhn et al. (2009); using coastal geomorphology and paleoseismic evidence, they documented a pattern of coastal uplift between Cape Yakataga and Icy Bay suggesting that a system of northeast-striking faults produced focused Quaternary uplift along the coastal exposures. They inferred that these structures connect to the offshore Pamplona fold-thrust belt, and that these structures are partially responsible for construction of the topographic high associated with the Dahlgren anticlinorium. Thus, these structures provide further support for the hypothesis that the Dahlgren anticlinorium, and the topographic high associated with it, are Quaternary features developed by out-of-sequence thrust systems and duplex formation at depth.

Collectively, these relationships support the conclusions of Chapman et al. (2008) and Berger et al. (2008a) that the Quaternary structure in the Duktoth area is dominated by a system of northeast-trending thrust systems (upper left, Fig. 13). The geometry of this array of

structures (Figs. 7 and 9; Supplemental Files 2 and 3 [see footnotes 2 and 3]). suggests that the modern kinematics of this segment of the orogen are dominated by dextral transpression along the en echelon fault array, with some slip transferred to offshore structures (Chapman et al., 2008). Nonetheless, it is conceivable this pattern is more directly tied to exhumation, and is simply a consequence of developing adjustments within the orogenic wedge. Some slip may also be transferred to a backthrust along the Bagley Icefield trough, but as noted above, this structural high could also be the backlimb of a regional antiformal stack developed above a duplex system (e.g., Fig. 10).

3D Processes in Icy Bay Transect

In the Icy Bay transect, there is a rich record of 3D complexities that vary in time, and although the details of these 3D effects are not yet well constrained, several features seem clear. Our geologic mapping (Plate 2) as well as the 3D visualization of those data (Fig. 9; Supplemental File 3 [see footnote 3]) illustrate that there is a systematic change in fold orientation with structural level and rock unit age throughout this area. In pre-Yakataga Formation strata, folds are either noncylindrical due to complex overprinting, or northwest trending, at a high angle to the deformation front of the currently active thrust, the Malaspina fault. Folds in synorogenic Yakataga strata, however, vary systematically from west-northwest trends in the Chaix Hills thrust sheet, to approximately east-west in the footwall of the Chaix Hills thrust sheet (Yakataga anticline and related folds), to east-west– to east-northeast–trending folds in the hanging wall of the Malaspina fault. This observation suggests strongly that the kinematic shortening axis in the Icy Bay region has rotated systematically in time from northeast trends to the present northwest trends. The simplest explanation for this change is not a change in shortening direction with time, but rather a kinematic response to the systematic transport of the Yakutat terrane into the tectonic corner of the eastern syntaxis (Chapman et al., 2012).

Synthesis

In Figure 13, we attempt to synthesize these relationships in a preliminary map-scale reconstruction of the region. The yellow shading represents gaps in the restoration, which represents active thrusts at the given time interval with shortening magnitudes estimated from our cross-section restorations (Figs. 10 and 11) and the offshore restorations of Worthington et al. (2010). The time intervals are based on the assumption that the Yakutat terrane moved with the Pacific plate and partitioning of convergence to the Denali fault system is equivalent to Holocene rates.

In the first step of this restoration, we restore ~1 m.y. of convergence as distributed deformation among thrust systems that are known or inferred to be active during this period. The offshore deformation is from the work of Worthington et al. (2010) and the onshore deformation is inferred from this study (upper right, Fig. 13). We infer that during this period, the northeast-trending thrusts warped their hanging walls to produce the younger, northwest-trending folds in the Duktoth region, and that a regional antiform grew to the north of these structures as a result of duplex formation. In the Icy Bay region, this period was accommodated by thrusting along the Malaspina fault, with some motion possibly accommodated on structurally higher faults (not shown) to produce the east-west– to northeast-trending fold systems (e.g., Yakataga anticline-syncline pair and the Samovar Hills anticline).

We then restore the thrust systems to ca. 2 Ma (lower left, Fig. 13); at this phase we restore the Chaix Hills thrust in the Icy Bay region as well as the Miller Creek fault in the Duktoth region. An important part of this restoration is that it carries the northwest-trending folds beneath the Coal Glacier thrust to a position that is essentially coincident with the syntaxis, where rapid kinematic changes are known or inferred from models (e.g., Koons et al., 2010). This restored position readily explains the apparent rotation in kinematic axes implied by differences in fold orientation across the basal Yakataga unconformity. That is, the fold in the Yakataga Formation records deformation in the syntaxis region that is kinematically distinct from older structures, indicating that the older structures formed prior to their arrival at the syntaxis.

We attempt to restore the system to ca. 5 Ma (lower right, Fig. 13). Because we cannot easily ascribe motion to specific structures during this time interval, this reconstruction is highly schematic; nonetheless, it shows three key features. First, the total shortening inferred in the Duktoth section can be accommodated as a broad band of convergence, including the virtual certainty that the leading edge of the suture (Chugach–St. Elias fault) was well south of its present position because erosion stripped away most of this material. Second, given recent work indicating that the Dangerous River zone (Fig. 13) is not a high-angle fault, but rather a shallow-dipping thrust placing the Yakutat Group on oceanic plateau basement (Worthington et al., 2012), we project a curved trace of the zone toward the interior of the orogen, illustrating how this paleogeography could account for extensive basement-involved thrust slices in the highest thrust sheets of the Icy Bay region (e.g., Haydon Peak assemblage). The restoration illustrates how the oldest, northwest-trending structures in the Icy Bay region restore to a position far south of the east-west–trending fold-thrust system in the interior of the orogen, indicating that these structures probably originated along the oblique, transpressional zone along the Fairweather fault, and were carried into their present position by tectonic transport.

General Implications for Tectonic Models of Eroding Orogenic Wedges

Theoretical models of orogenic wedges predict that if the surface slope is decreased the taper of the wedge will adjust by internal deformation (e.g., Dahlen, 1990). This conclusion is supported through analog and numerical models (e.g., Koons, 1989; Beaumont et al., 1992; Willett, 1999), including those specific to glacial erosion (Tomkin, 2007; Tomkin and Roe, 2007). Along-strike variations in structural geology and the history of sedimentation allow us to further explore this process in the St. Elias orogen. In the east, the thrust belt is youngest because material is rafted into the syntaxis along the Fairweather transform fault, but progressing westward the orogen records an increasingly long record of convergence that is superimposed on the transpressional structures that develop adjacent to the transform boundary (e.g., Fig. 13). The bulk of the rocks now involved in the fold-thrust system at Icy Bay were carried into the syntaxis in the past ~2–3 m.y. (Fig. 13), with structures inherited from a modest component of transpression along the Fairweather fault. Thus, the Icy Bay region serves as a proxy for a young convergent orogen, but one where the mass flux to the thrust front is large because the combined thickness of sedimentary deposits overlying deformed strata is as much as 10 km where it enters the subduction system. This structural configuration produces a rapid growth of the orogenic wedge out into the orogenic foreland and rapid uplift within the wedge if erosion is vigorous (e.g., analog physical modeling by Malavieille, 1010; Konstantinovskaya and Malavieille, 2011). Geodetic studies (Elliott, 2011) indicate that most of the deformation is transferred directly to the deformation front (Malaspina fault and other faults concealed beneath the Malaspina Glacier); less than half of the deformation is transferred to internal deformation of the orogenic wedge. Erosion within the orogenic wedge is accompanied by rapid uplift, erosion, and development of out-of-sequence faults that indicate that restoration of the wedge taper is ongoing (Plate 1; e.g., Enkelmann et al., 2009, 2010).

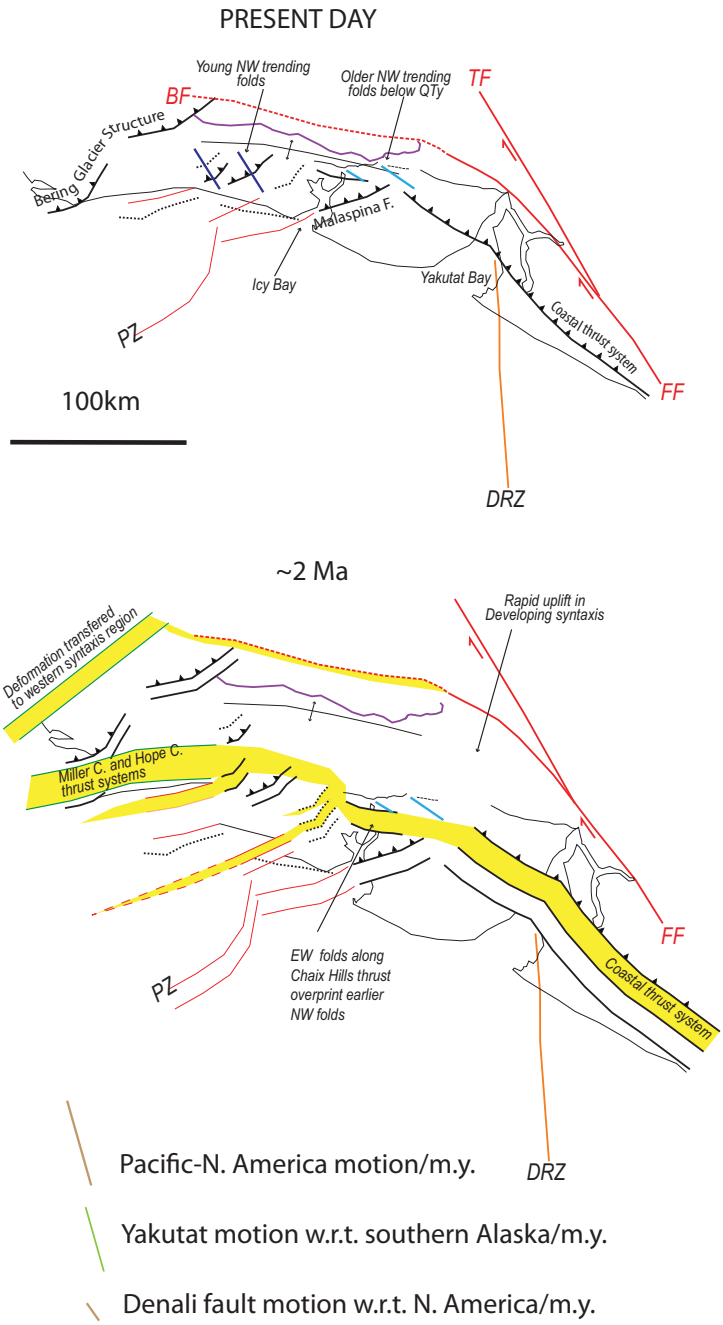

Figure 13 (*continued on following page*). Map-scale reconstruction using major structures from Figure 2 together with cross-section restorations to infer a paleogeography through time. Time is inferred from an assumption that full Pacific–North American convergence is transferred to southern Alaska through a combination of convergence in the orogen and strike-slip on the Denali fault system at Holocene rates. Yellow areas show reconstruction gaps interpreted as areas of shortening during each time interval. Future areas of shortening are carried through in the restoration to older time periods; colors are carried through the restoration. Figure shows four time slices: present day (upper left), 1 Ma (upper right), 2 Ma (lower left), and 5 Ma (lower right) with plate and microplate motions in lower left scaled to 1 m.y. of motion. The restoration becomes increasingly speculative with increased time, but the 1 Ma is relatively well constrained by results reported here and in Worthington et al. (2010). Note how the 2 Ma and 5 Ma panels show restoration of the northwest-trending folds in the Icy Bay region (blue lines) into the foreland of the oblique-transpressional part of the orogen, and restore the Dangerous River zone (DRZ) to a configuration consistent with Yakutat Group basement exposures in the Mount St. Elias region. Also note the inferred origin of the northwest-trending, younger folds in the Duktoth area (dark blue lines) as secondary structures along out-of-sequence, northeast-trending thrusts formed in last 1 m.y. of the orogen. Abbreviations: Qty—Yakutaga Formation; F.—fault; C.—Creek; CSEF—Chugach–St. Elias fault; BF—Bagley fault; FF—Fairweather fault; PZ—Pamplona zone; TF—Totschunda fault; NW—northwest; EW—east-west; w.r.t.—with respect to; ss—strike-slip.

The thrust belt widens toward the west because of a longer history of greater convergence within the central, or Yakataga, segment of the orogen, but crustal loading by the accumulation of sedimentary deposits offshore apparently dampens tectonic activity by increasing the vertical tectonic stress (e.g., Worthington et al., 2010). Only 10%–20% of the late Pleistocene to recent convergence is taken up by offshore structures; the remaining 80%–90% of the convergence is presumably accommodated in the onshore fold-thrust belt. This conclusion is supported by geodetic studies (Elliott, 2011) that suggest dispersed deformation through this region. These and other structural observations (cited in the previous paragraph) lead us to propose that the deformation within the central part of the thrust belt is distributed across several faults, with most of that deformation concentrated in mountains onshore (Fig. 13). These out-of-sequence thrusts, together with the offshore structures, transfer slip downdip into the duplex system that produces a vertically growing antiformal stack beneath the coastal mountains. This antiformal stack drives the long-term uplift and exhumation that is recorded in thermochronology data (Spotila and Berger, 2010; Enkelmann et al., 2010) and, for example, creates the tectonic highland that extends across the foreland thrust belt immediately west of Icy Bay (Bruhn et al., 2009).

These generalizations about this tectonic system yield more insights through compari-

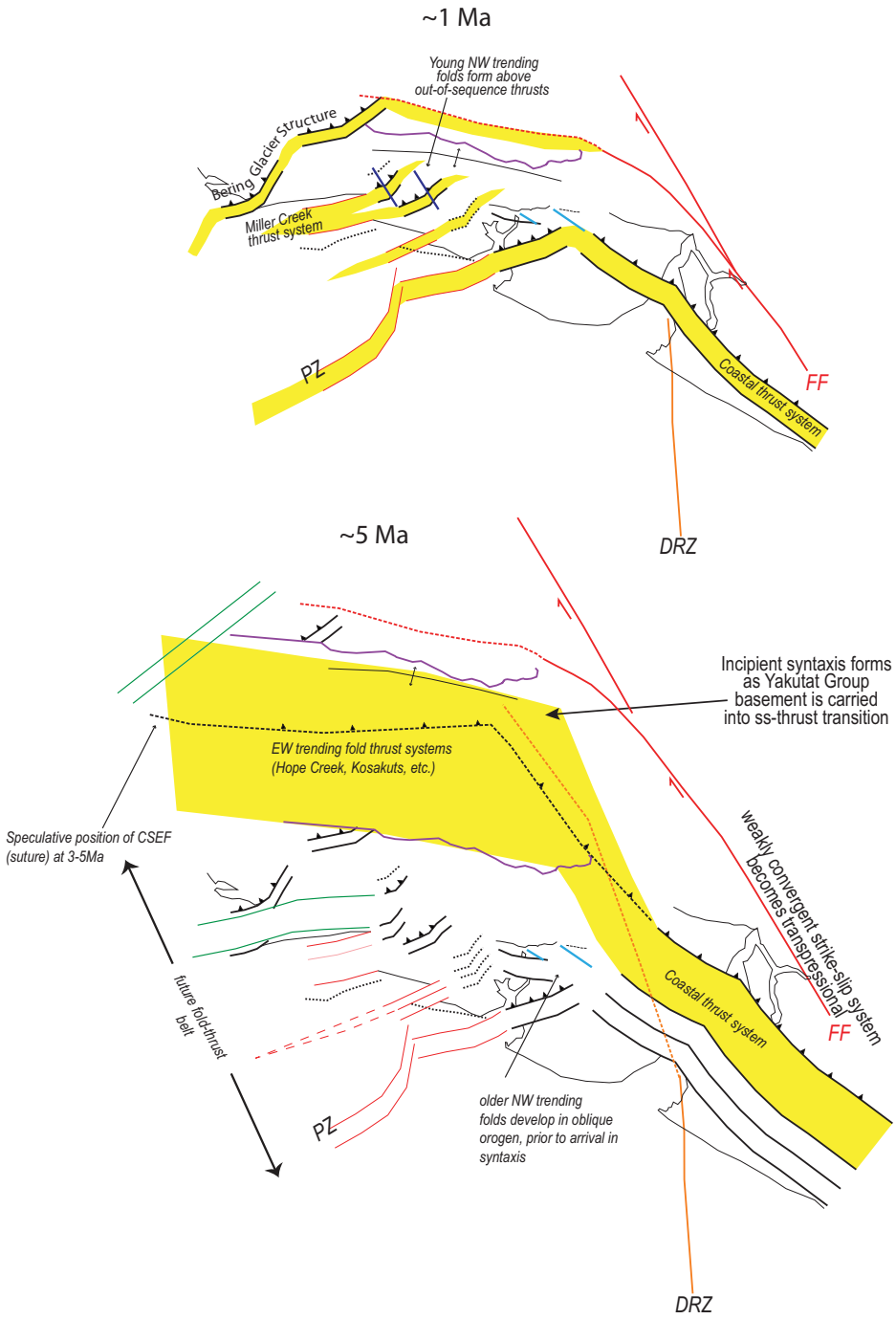

son to recent modeling studies. Analog models of Konstantinovskaya and Malavieille (2005, 2011) indicate that growth of an antiformal duplex is characteristic of an orogen where erosion keeps pace with uplift. However, models where sedimentary deposition outpaces erosion (Simpson, 2010) produce structures that are similar to the discrete fault-propagation folds that are developed offshore (Worthington et al., 2010). We suggest that these models together represent a reasonable proxy for the more mature, central segment of the St. Elias orogen (e.g., Fig. 10). That is, part of the deformation in transferred to offshore structures, outboard of a major sedimentary basin that developed late in the history of the orogen (e.g., Berger et al., 2008; Worthington et al., 2010) as in sedimentary models of Simpson (2010) and the remainder of the deformation is transferred to onshore structure by processes like those in the models of Konstantinovskaya and Malavieille (2005, 2011). We speculate that this combination of processes is a natural consequence of an orogenic system that was fundamentally reshaped in the Pleistocene through rapid erosion of the onshore orogen with sediment deposited immediately offshore. We suggest that future modeling studies need to examine the hypothesis that this orogenic system is responding to a major redistribution of mass in the past 1–2 m.y., when sediment eroded from mountains was transported and deposited in the adjacent offshore region.

CONCLUSIONS

The Yakataga segment of the St. Elias orogen is characterized by 3D structure that evolved in time due to the transport of the Yakutat terrane into the tectonic corner of the St. Elias orogen. Simplification of the 3D architecture to a pair of cross sections can account for 150–200 km of convergence, only a fraction of the probable total collisional convergence. Based on regional geophysical observations and mass discrepancies, we suggest that much of this missing convergence was accommodated by sediment subduction, and future studies need to address this question.

Different 3D processes have shaped the two transects of the Yakataga fold-thrust belt. In the Duktoth transect, we infer a transition in time from typical stacked fold-thrust belt to development of an array of out-of-sequence fold-thrust systems. Based on cross-section construction, we suggest that this young thrust system passes downward into an antiformal stack beneath the site of maximum exhumation, as recorded in thermochronology data (Spotila and Berger, 2010). By analogy with model results of Malavieille (2010) and Konstantinovskaya and Malavieille (2005, 2011), this structural geometry is a natural consequence of a rapidly eroding orogenic wedge with a weak layer in the stratigraphic assemblage. We infer that coal-bearing strata of the middle Kulthieth Formation provided the weak layer in the St. Elias orogen, and efficient glacial erosion produced exhumation sufficient to maintain the antiformal structure. We envision a more complex system in the Icy Bay region related to transport of material from the oblique-convergent part of the orogen into the fully convergent Yakataga fold-thrust belt, a history consistent with the complex kinematic changes predicted for geodynamics models of this type of tectonic corner (as in models of Koons et al., 2010). Collectively, along-strike variations in structure within the fold-thrust system represent a classic trade-off in space for time and show how orogenic structures change during accumulated convergence under the influence of intense erosion and deposition.

ACKNOWLEDGMENTS

This work was conducted as part of the St. Elias Erosion and Tectonics Project (STEEP) sponsored by the Continental Dynamics Program of the National Science Foundation (NSF). This support includes NSF grants EAR-0409009, EAR-0735402, and EAR-1009533 to Pavlis, EAR-0409009 and EAR-1009584 to Bruhn, EAR-0910945 and EAR-0409299 to Ridgway, EAR-0408584 and EAR-1009986 to Gulick, and EAR-0409224 and EAR-1009845 to Spotila. We thank all members of this research team for discussions of the results reported in this paper, particularly those who contributed as yet unpublished information that is used peripherally in this paper. Reviews by Andrew Meigs, Deta Gasser, Peter Haeussler, and Kurt Stuwe provided valuable input for improving the manuscript. This is University of Texas Institute for Geophysics (UTIG) contribution 2466.

We thank George Plafker for sharing his field map sheets from years of work in this region as well as for working with us in the field during two of the field seasons. We also thank Mike Vorkink for sharing his field data, Peter Haeussler for volunteering time in the field effort, and Evan Toms for his input with field data acquisition systems we used in the first year of this project. We also thank the staff at Midland Valley Ltd. for technical support with Move software, the Resource Management staffs at Wrangell–St. Elias National Park and Preserve and Chugach National Forest for their help in permitting this project, and the Anchorage Bureau of Land Management staff for logistical assistance in the first year of this project.

REFERENCES CITED

Alley, R.B., Lawson, D.E., Larson, G.J., Evenson, E.B., and Baker, G.S., 2003, Stabilizing feedbacks in glacier-bed erosion: Nature, v. 424, p. 458–460, doi:10.1038/nature01839.

Arnaud, E., 2010, Onset of late Cenozoic glaciation in the Gulf of Alaska: Geological Society of America Abstracts with Programs, v. 42, no. 5, p. 361.

Arnold, L., 2010, Metamorphic trends of the St. Elias Range, southeast Alaska [thesis]: El Paso, University of Texas at El Paso.

Beaumont, C., Fullsack, P., and Hamilton, J., 1992, Erosional control of active compressional orogens, *in* McKay, K., ed., Thrust tectonics: Boca Raton, Florida, CRC Press, p. 1–18.

Benowitz, J.A., Layer, P.W., Armstrong, P., Perry, S.E., Haeussler, P.J., Fitzgerald, P.G., and VanLaningham, S., 2011, Spatial variations in focused exhumation along a continental-scale strike-slip fault: The Denali fault of the eastern Alaska Range: Geosphere, v. 7, p. 455–467, doi:10.1130/GES00589.1.

Berger, A.L., and Spotila, J.A., 2008, Denudation and deformation of a glaciated orogenic wedge: The St. Elias orogen, Alaska: Geology, v. 36, p. 523–526, doi:10.1130/G24883A.1.

Berger, A.L., Spotila, J., Chapman, J., Pavlis, T., Enkelmann, E., and Buscher, J., 2008a, Architecture, kinematics, and exhumation of a convergent wedge: A thermochronological investigation of tectonic-climatic interactions within the central St. Elias Orogen, Alaska: Earth and Planetary Science Letters, v. 270, p. 13–24, doi:10.1016/j.epsl.2008.02.034.

Berger, A.L., Gulick, S.P., Spotila, J.A., Upton, P., Jaeger, J.M., Chapman, J.B., Worthington, L., Pavlis, T.L., Ridgway, K.R., Willems, B., and McAleer, A., 2008b, Quaternary tectonic response to intensified glacial erosion in an orogenic wedge: Nature Geoscience, v. 1, p. 793–799, doi:10.1038/ngeo334.

Broadwell, M.S., 2001, Geometry and kinematics of the Yakataga anticline, Icy Bay, Alaska [M.S. thesis]: Fairbanks, University of Alaska, 76 p.

Brocklehurst, S.H., and Whipple, K.X., 2002, Glacial erosion and relief production in the eastern Sierra Nevada, California: Geomorphology, v. 42, p. 1–24, doi:10.1016/S0169-555X(01)00069-1.

Brozovic, N., Burbank, D.W., and Meigs, A.J., 1997, Climatic limits on landscape development in the northwestern Himalaya: Science, v. 276, p. 571–574, doi:10.1126/science.276.5312.571.

Bruand, E., 2011, A petrological study of the Chugach metamorphic complex in southern Alaska [Ph.D. thesis]: Graz, Austria, Karl Franzens University, 204 p.

Bruand, E., Gasser, D., Bonnand, P., and Stuewe, K., 2011, The petrology and geochemistry of a metabasite belt along the southern margin of Alaska: Lithos, v. 127, p. 282–297, doi:10.1016/j.lithos.2011.07.026.

Bruhn, R.L., Pavlis, T.L., Plafker, G., and Serpa, L., 2004, Deformation during terrane accretion in the Saint Elias orogen, Alaska: Geological Society of America Bulletin, v. 116, p. 771–787, doi:10.1130/B25182.1.

Bruhn, R., Shennan, I., Plafker, G., Pavlis, T.L., and Chapman, J.V., 2009, Coastal deformation in the northeastern Gulf of Alaska, Saint Elias orogen: Great earthquakes, active structures, and glacial fluctuations: Geological Society of America Abstracts with Programs, v. 41, no. 7, p. 185.

Bruhn, R.L., Forster, R.R., Ford, A.A., Pavlis, T.L., and Vorkink, M., 2010, Structural geology and glacier dynamics, Bering and Stellar Glaciers, Alaska, *in* Shuchman, R.A., and Josberger, E.G., eds., Bering Glacier: Interdisciplinary studies of Earth's largest temperate surging glacier: Geological Society of America Special Paper 462, p. 217–233, doi:10.1130/2010.2462(11).

Bruns, T.R., and Schwab, W.C., 1983, Structure maps and seismic stratigraphy of the Yakataga segment of the continental margin, northern Gulf of Alaska: U.S. Geological Survey Miscellaneous Field Studies Map MF-1424, 25 p.

Campbell, R.B., and Dodds, C.J., 1982, Geology of the Mount St. Elias map area (115B and 115C) Yukon Territory: Geological Survey of Canada Open File Report 830, scale 1:250,000.

Chapman, J.B., 2008, Structural relationships and crustal deformation in the Saint Elias Orogen, Alaska [M.S. thesis]: El Paso, University of Texas, no. 6542, http://lib.utep.edu/search/Y?SEARCH=chapman+alaska+thesis.

Chapman, J.B., and 14 others, 2008, Neotectonics of the Yakutat collision: Changes in deformation driven by mass redistribution, *in* Freymueller, J.T., et al., eds., Tectonics and seismic hazards of Alaska: American Geophysical Union Geophysical Monograph 179, p. 65–81, doi:10.1029/179GM04.

Chapman, J.B., Worthington, L.L., Pavlis, T.L., Bruhn, R.L., Gulick, S.P., 2011, The Suckling Hills fault, Kayak Island Zone, and accretion of the Yakutat microplate, Alaska: Tectonics, v. 30, TC6011, doi:10.1029/2011TC002945.

Chapman, J.B., Pavlis, T.L., Bruhn, R.L., Worthington, L.L., Gulick, S.P.S., and Berger, A.L., 2012, Structural relationships in the eastern syntaxis of the Saint Elias orogen, Alaska: Geosphere, v. 8, p. 105–126, doi:10.1130/GES00677.1.

Cotton, M.M., Bruhn, R.L., Sauber, J.M., and Burgess, E.W., 2011, Remote sensing and modeling of sub-glacier geomorphology: The role geological structures play in controlling the geometry and dynamics of ice flow on the Malaspina Glacier, AK: American Geophysical Union, fall meeting 2011, abs. C53B-0670.

Dahlen, F.A., 1990, Critical taper model of fold-and-thrust belts and accretionary wedges: Annual Review of Earth and Planetary Sciences, v. 18, p. 55–99, doi:10.1146/annurev.ea.18.050190.000415.

Eberhart-Phillips, D., Christensen, D.H., Brocher, T.M., Hansen, R., Ruppert, N.A., Haeussler, P.J., and Abers, G.A., 2006, Imaging the transition from Aleutian subduction to Yakutat collision in central Alaska, with local earthquakes and active source data: Journal of Geophysical Research, v. 111, B11303, doi:10.1029/2005JB004240.

Elliott, J., 2011, Active tectonics in southern Alaska and the role of the Yakutat block constrained by GPS measurements [Ph.D. thesis]: Fairbanks, University of Alaska, 187 p.

Elliott, J.L., Larsen, C.F., Freymueller, J.T., and Motyka, R.J., 2010, Tectonic block motion and glacial isostatic adjustment in southeast Alaska and adjacent Canada constrained by GPS measurements: Journal of Geophysical Research, v. 115, B09407, doi:10.1029/2009JB007139.

Enkelmann, E., Garver, J.I., and Pavlis, T.L., 2008, Rapid exhumation of ice-covered rocks in the Chugach–St. Elias orogen, southeast Alaska: Geology, v. 36, p. 915–918, doi:10.1130/G2252A.1.

Enkelmann, E., Zeitler, P.K., Pavlis, T.L., Garver, J.I., and Ridgway, K.D., 2009, Intense localized rock uplift and erosion in the St. Elias orogen of Alaska: Nature Geoscience, v. 2, p. 360–363, doi:10.1038/ngeo502.

Enkelmann, E., Zeitler, P.K., Garver, J.I., Pavlis, T.L., and Hooks, B., 2010, The thermochronological record of tectonic and surface process interaction at the Yakutat–North American collision zone in southeast Alaska: American Journal of Science, v. 310, p. 231–260, doi:10.2475/04.2010.01.

Estabrook, C.H., Nabelek, J.L., and Lerner-Lam, A.L., 1992, Tectonic model of the Pacific–North American plate boundary in the Gulf of Alaska from broadband analysis of the 1979 St. Elias, Alaska, earthquake and aftershocks: Journal of Geophysical Research, v. 97, p. 6587–6612, doi:10.1029/92JB00131.

Eyles, C.H., Eyles, N., and Lagoe, M.B., 1991, The Yakataga Formation, a late Miocene to Pleistocene record of temperate glacial marine sedimentation in the Gulf of Alaska, *in* Anderson, J.B., and Ashley, G.M., eds., Glacial-marine sedimentation; Paleoclimatic significance: Geological Society of America Special Paper 261, p. 159–180.

Ferris, A., Abers, G.A., Christensen, D.H., and Veenstra, E., 2003, High resolution image of the subducted Pacific plate beneath central Alaska, 50–150 km depth: Earth and Planetary Science Letters, v. 214, p. 575–588, doi:10.1016/S0012-821X(03)00403-5.

Finzel, E.S., Trop, J.M., Ridgway, K.D., and Enkelmann, E., 2011, Upper plate proxies for flat-slab subduction processes in southern Alaska: Earth and Planetary Science Letters, v. 303, p. 348–360, doi:10.1016/j.epsl.2011.01.014.

Freymueller, J.T., Woodard, H., Cohen, S.C., Cross, R., Elliot, J., Larsen, C.F., Hreinsdottir, S., and Zweck, C., 2008, Active deformation processes in Alaska, based on 15 years of GPS measurements, *in* Freymueller, J.T., et al., eds., Tectonics and seismic hazards of Alaska: American Geophysical Union Geophysical Monograph 179, p. 1–42, doi:10.1029/179GM02.

Fruehn, J., Von Huene, R., and Fisher, M.A., 1999, Accretion in the wake of terrane collision: The Neogene accretionary wedge off Kenai Peninsula, Alaska: Tectonics, v. 18, p. 263–277, doi:10.1029/1998TC900021.

Fuis, G.S., Ambos, E.L., Mooney, W.D., Christensen, N.I., and Geist, E., 1991, Crustal structure of accreted terranes in southern Alaska, Chugach Mountains and Copper River basin, from seismic refraction results: Journal of Geophysical Research, v. 96, p. 4187–4227, doi:10.1029/90JB02316.

Gasser, D., Bruand, E., Stüwe, K., Foster, D., Schuster, R., Fügenschuh, B., and Pavlis, T., 2011, Formation of a metamorphic complex along an obliquely convergent margin: Structural and thermochronological evolution of the Chugach Metamorphic Complex, southern Alaska: Tectonics, v. 30, 25 p., doi:10.1029/2010TC002776.

Griffiths, T.M., 1952, Glacial geomorphology on the Mt. McKinley massif, Alaska, *in* Proceedings, eighth general assembly and seventeenth international congress, International Geographical Union: Washington, D.C., International Geographical Union, p. 331–336.

Hacker, B.R., Abers, G.A., and Peacock, S.M., 2003, Subduction factory 1. Theoretical mineralogy, densities, seismic wave speeds, and H_2O contents: Journal of Geophysical Research, v. 108, no. B1, 2029, doi:10.1029/2001JB001127.

Haeussler, P.J., 2008, An overview of the neotectonics of interior Alaska: Far field deformation from the Yakutat microplate collision, *in* Freymueller, J.T., et al., eds., Tectonics and seismic hazards of Alaska: American Geophysical Union Geophysical Monograph 179, p. 83–108, doi:10.1029/179GM05.

Hallet, B., 1979, A theoretical model of glacial abrasion: Journal of Glaciology, v. 23, p. 29–50.

Hallet, B., Hunter, L., and Bogen, J., 1996, Rates of erosion and sediment evacuation by glaciers: A review of field data and their implications: Global and Planetary Change, v. 12, p. 213–235, doi:10.1016/0921-8181(95)00021-6.

Jaeger, J.M., Nitrouer, C.A., Scott, N.D., and Milliman, J.D., 1998, Sediment accumulation along a glacially impacted mountainous coastline—North-east Gulf of Alaska: Basin Research, v. 10, p. 155–173, doi:10.1046/j.1365-2117.1998.00059.x.

Konstantinovskaya, E.A., and Malavieille, J., 2005, Erosion and exhumation in accretionary orogens: Experimental and geological approaches: Geochemistry Geophysics Geosystems, v. 6, Q02006, doi:10.1029/2004GC000794.

Konstantinovskaia, E., and Malavieille, J., 2011, Thrust wedges with decollement levels and syntectonic erosion: A view from analog models: Tectonophysics, v. 502, p. 336–350, doi:10.1016/j.tecto.2011.01.020.

Koons, P.O., 1989, The topographic evolution of collisional mountain belts: A numerical look at the southern Alps, New Zealand: American Journal of Science, v. 289, p. 1041–1069, doi:10.2475/ajs.289.9.1041.

Koons, P.O., Hooks, B.P., Pavlis, T., Upton, P., and Barker, A.D., 2010, Three-dimensional mechanics of Yakutat convergence in the southern Alaskan plate corner: Tectonics, v. 29, TC4008, doi:10.1029/2009TC002463.

Lagoe, M.B., Eyles, C.H., Eyles, N., and Hale, C., 1993, Timing of late Cenozoic tidewater glaciation in the far north Pacific: Geological Society of America Bulletin, v. 105, p. 1542–1560, doi:10.1130/0016-7606(1993)105<1542:TOLCTG>2.3.CO;2.

Landis, P., 2007, Stratigraphic framework and provenance of the Eocene-Oligocene Kulthieth Formation, Alaska: Implications for paleogeography and tectonics of the early Cenozoic continental margin of northwestern North America [M.S. thesis]: West Lafayette, Indiana, Purdue University, 200 p.

Lull, J.S., and Plafker, G., 1990, Geochemistry and paleotectonic implications of metabasaltic rocks in the Valdez Group, southern Alaska, *in* Dover J.H., and Galloway, J.P., eds., Geologic studies in Alaska by the U.S. Geological Survey in 1989: U.S. Geological Survey Bulletin 1946, p. 29–38.

MacGregor, K.R., Anderson, R.S., Anderson, S.P., and Waddington, E.D., 2000, Numerical simulations of glacial-valley longitudinal profile evolution: Geology, v. 28, p. 1031–1034, doi:10.1130/0091-7613(2000)28<1031:NSOGLP>2.0.CO;2.

Malavieille, J., 2010, Impact of erosion, sedimentation, and structural heritage on the structure and kinematics of orogenic wedges: Analog models and case studies: GSA Today, v. 20, p. 4–10, doi:10.1130/GSATG48A.1.

Martin, G.C., 1992, Part I: Regional geology, lithostratigraphy, *in* Turner, R.F., ed., Geologic report for the Gulf of Alaska planning area: U.S. Minerals Management Service Outer Continental Shelf Report MMS 92–0065, p. 63–98.

Mazzotti, S., and Hyndman, R.D., 2002, Yakutat collision and strain transfer across the northern Canadian Cordillera: Geology, v. 30, p. 495–498, doi:10.1130/0091-7613(2002)030<0495:YCASTA>2.0.CO;2.

Meigs, A., and Sauber, J., 2000, Southern Alaska as an example of the long-term consequences of mountain building under the influence of glaciers: Quaternary Science Reviews, v. 19, p. 1543–1562, doi:10.1016/S0277-3791(00)00077-9.

Meigs, A., Johnston, S., Garver, J., and Spotila, J., 2008, Crustal-scale structural architecture, shortening, and exhumation of an active eroding orogenic wedge (the Chugach/St. Elias Range, southern Alaska): Tectonics, v. 27, TC4003, doi:10.1029/2007TC002168.

Miller, D.J., 1957, Geology of the southeastern part of the Robinson Mountains, Yakataga District, Alaska: U.S. Geological Survey Oil and Gas Investigations Map OM-187, 2 sheets, scale 1:63,360.

Miller, D.J., 1971, Geologic map of the Yakataga district, Gulf of Alaska Tertiary province, Alaska: U.S. Geological Survey Miscellaneous Geologic Investigations Map I-610, scale 1:125,000.

Miller, D.J., 1975, Geologic map and sections of the central part of the Katalla district, Alaska: U.S. Geological Survey Miscellaneous Field Studies Map MF-722, scale 1:40,000.

Montgomery, D.R., 2002, Valley formation by fluvial and glacial erosion: Geology, v. 30, p. 1047–1050, doi:10.1130/0091-7613(2002)030<1047:VFBFAG>2.0.CO;2.

Pavlis, T.L., and Bruhn, R.L., 1983, Deep-seated flow as a mechanism for the uplift of broad forearc ridges and its role in the exposure of high P/T metamorphic terranes: Tectonics, v. 2, p. 473–497, doi:10.1029/TC002i005p00473.

Pavlis, T.L., Hamburger, M.W., and Pavlis, G.L., 1997, Erosional processes as a control on the structural evolution of an actively deforming fold and thrust belt: An example from the Pamir-Tien Shan region, central Asia: Tectonics, v. 16, p. 810–822, doi:10.1029/97TC01414.

Pavlis, T.L., Picornell, C., Serpa, L., Bruhn, R.L., and Plafker, G., 2004, Tectonic processes during oblique collision: Insights from the St. Elias orogen, northern North American Cordillera: Tectonics, v. 23, TC3001, doi:10.1029/2003TC001557.

Pavlis, T.L., Langford, R., Hurtado, J., and Serpa, L., 2010, Computer-based data acquisition and visualization systems in field geology: Results from 12 years of, experimentation and future potential: Geosphere, v. 6, p. 275–294, doi:10.1130/GES00503.1.

Plafker, G., 1967, Geologic map of the Gulf of Alaska Tertiary Province: U.S. Geological Survey Miscellaneous Geologic Investigations Map I-484, scale 1:500,000.

Plafker, G., 1971, Possible future petroleum resources of Pacific margin Tertiary basin, Alaska, *in* Cram, I.H., ed., Future petroleum provinces of the United States—Geology and potential: American Association of Petroleum Geologists Memoir 15, v. 1, p. 120–135.

Plafker, G., 1987, Regional geology and petroleum potential of the northern Gulf of Alaska, *in* Scholle, D.W., et al., eds., Geology and resource potential of the continental margin of the western North American and adjacent ocean basins—Beaufort Sea to Baja California: Circum-Pacific Council for Energy and Mineral Resources Earth Science Series 6, p. 229–268.

Plafker, G., and Addicott, W.O., 1976, Glaciomarine deposits of Miocene through Holocene age in the Yakataga Formation along the Gulf of Alaska margin, *in* Miller, T.P., ed., Recent and ancient sedimentary environments in Alaska: Alaska Geological Society Symposium Proceedings, p. Q1–Q23.

Plafker, G., and Miller, D.J., 1957, Reconnaissance geology of the Malaspina District, Alaska: U.S. Geological Survey Oil and Gas Investigations Map OM-189, scale 1:125,000.

Plafker, G., Bruns, T.R., and Page, R.A., 1975, Interim report on petroleum resource potential and geologic hazards in the outer continental shelf of the Gulf of Alaska Tertiary province: U.S. Geological Survey Open-File Report 75–592, 74 p.

Plafker, G., Moore, J.C., and Winkler, G.R., 1994, Geology of the southern Alaska margin, *in* Plafker, G., and Berg, H.C., eds., The Geology of Alaska: Boulder, Colorado, Geological Society of America, The Geology of North America, v. G-1, p. 389–449.

Richter, D.H., Preller, C.C., Labay, K.A., and Shew, N.B., 2006, Geology of Wrangell–Saint Elias National Park and Preserve, south-central Alaska: U.S. Geological Survey Scientific Investigations Series Map SIM-2877, scale 1:350,000.

Risley, D.E., 1992, Part I: Regional geology, structural geology, *in* Turner, R.F., ed., Geologic report for the Gulf of Alaska planning area: U.S. Minerals Management Service Outer Continental Shelf Report MMS 92–0065, p. 45–62.

Rossi, G., Abers, G.A., Rondenay, S., and Christensen, D.H., 2006, Unusual mantle Poisson's ratio, subduction, and crustal structure in central Alaska: Journal of Geophysical Research, v. 111, B09311, doi:10.1029/2005JB003956.

Scharman, M.R., Pavlis, T.L., Day, E.M., and O'Driscoll, L.J., 2011, Deformation and structure in the Chugach metamorphic complex, southern Alaska: Crustal architecture of a transpressional system from a down plunge section: Geosphere, v. 7, p. 992–1012, doi:10.1130/GES00646.1.

Sheaf, M., Serpa, L., and Pavlis, T., 2003, Exhumation rates in the St. Elias Mountains, Alaska: Tectonophysics, v. 367, p. 1–11, doi:10.1016/S0040-1951(03)00124-0.

Simpson, G.D.H., 2010, Formation of accretionary prisms influenced by sediment subduction and supplied by sediments from adjacent continents: Geology, v. 38, p. 131–134, doi:10.1130/G30461.1.

Spotila, J.A., and Berger, A.L., 2010, Exhumation at orogenic indentor corners under long-term glacial conditions: Example of the St. Elias orogen, Southern Alaska: Tectonophysics, v. 490, p. 241–256, doi:10.1016/j.tecto.2010.05.015.

Tomkin, J.H., 2007, Coupling glacial erosion and tectonics at active orogens: A numerical modeling study: Journal of Geophysical Research, v. 112, F02015, doi:10.1029/2005JF000332.

Tomkin, J.H., and Roe, G.H., 2007, Climate and tectonic controls on glaciated critical-taper orogens: Earth and Planetary Science Letters, v. 262, p. 385–397, doi:10.1016/j.epsl.2007.07.040.

Wallace, W.K., 2008, Yakataga fold-and-thrust belt: Structural geometry and tectonic implications of a small continental collision zone, *in* Freymueller, J.T., et al., eds., Tectonics and seismic hazards of Alaska: American Geophysical Union Geophysical Monograph 179, p. 237–256, doi:10.1029/179GM13.

Whipple, K.X., 2009, The influence of climate on the tectonic evolution of mountain belts: Nature Geoscience, v. 2, p. 97–104, doi:10.1038/ngeo413.

Wilson, F.H., Labay, K.A., Shew, N.B., Preller, C.C., Mohadjer, S., and Richter, D.H., 2005, Preliminary integrated geologic map databases for the United States: Digital data for the geology of Wrangell–Saint Elias National Park and Preserve, Alaska: U.S. Geological Survey Open-File Report 2005–1342, http://pubs.usgs.gov/of/2005/1342/.

Willett, S.D., 1999, Orogeny and orography: The effects of erosion on the structure of mountain belts: Journal of Geophysical Research, v. 104, p. 28,957–28,981, doi:10.1029/1999JB900248.

Witmer, J.W., 2009, Neogene deposition, provenance, and exhumation along a tectonically active, glaciated continental margin, Yakataga and Redwood Formations, southern Alaska syntaxis [M.S. thesis]: West Lafayette, Indiana, Purdue University, 313 p.

Worthington, L.L., Gulick, S.P., and Pavlis, T.L., 2008, Identifying active structures in the Kayak Island and Pamplona Zones: Implications for offshore tectonics of the Yakutat microplate, Gulf of Alaska, *in* Freymueller, J.T., et al., eds., Tectonics and seismic hazards of Alaska: American Geophysical Union Geophysical Monograph 179, p. 257–268, doi:10.1029/179GM14.

Worthington, L.L., Gulick, S.P.S., and Pavlis, T.L., 2010, Coupled stratigraphic and structural evolution of a glaciated orogenic wedge, offshore St. Elias Orogen, Alaska: Tectonics, v. 29, TC6013, doi:10.1029/2010TC002723.

Worthington, L.L., Van Avendonk, H.J.A., Gulick, S.P.S., Christeson, G.L., and Pavlis, T.L., 2012, Crustal structure of the Yakutat terrane and the evolution of subduction and collision in southern Alaska: Journal of Geophysical Research, v. 117, B01102, doi:10.1029/2011JB008493.

Ye, S., Flueh, E.R., Kaeschen, D., and Von Huene, R., 1997, Crustal structure along the EDGE transect beneath the Kodiak Shelf off Alaska derived from OBH seismic refraction data: Geophysical Journal International, v. 130, p. 283–302, doi:10.1111/j.1365-246X.1997.tb05648.x.

Zellers, S.D., 1995, Foraminiferal sequence biostratigraphy and seismic stratigraphy of a tectonically active margin; the Yakataga Formation, northeastern Gulf of Alaska: Marine Micropaleontology, v. 26, p. 255–271, doi:10.1016/0377-8398(95)00031-3.